Emergence of spacetime in a restricted spin-foam model

Sebastian Steinhaus*
Perimeter Institute for Theoretical Physics, 31 Caroline Street North, Waterloo, N2L 2Y5 Ontario, Canada

Johannes Thürigen†
Department of Physics, Department of Mathematics, Humboldt-Universität zu Berlin, Unter den Linden 6,10099 Berlin, Germany

(Received 16 April 2018; published 9 July 2018)

The spectral dimension has proven to be a very informative observable to understand the properties of quantum geometries in approaches to quantum gravity. In loop quantum gravity and its spin-foam description, it has not been possible so far to calculate the spectral dimension of spacetime. As a first step towards this goal, here we determine the spacetime spectral dimension in the simplified spin-foam model restricted to hypercuboids. Using Monte Carlo methods we compute the spectral dimension for state sums over periodic spin-foam configurations on infinite lattices. For given periodicity, i.e. number of degrees of freedom, we find a range of scale where an intermediate spectral dimension between 0 and 4 can be found, continuously depending on the parameter of the model. Under an assumption on the statistical behavior of the Laplacian we can explain these results analytically. This allows us to take the thermodynamic limit of large periodicity and find a phase transition from a regime of effectively zero-dimensional to four-dimensional spacetime. At the point of phase transition, dynamics of the model are scale invariant which can be seen as restoration of diffeomorphism invariance of flat space. Considering the spectral dimension as an order parameter for renormalization we find a renormalization group flow to this point as well. Being the first instance of an emergence of four-dimensional spacetime in a spin-foam model, the properties responsible for this result seem to be rather generic. We thus expect similar results for more general, less restricted spin-foam models.

DOI: 10.1103/PhysRevD.98.026013

I. INTRODUCTION

Any approach of quantum gravity that replaces the continuous metric for a postulated fundamental, often discrete, structure has to face the challenge to connect back to well-known continuum physics, in particular, a smooth four-dimensional spacetime. Often it is argued that such a spacetime should "emerge" from this quantum theory in a suitable continuum limit [1–4]. While this is an appealing picture, defining and performing such a continuum limit is the essential point of ongoing research. Moreover, a theory of quantum gravity may allow for many different phases resulting in very different continuum spacetimes. To gain an insight and better understanding of the dynamics of such a theory, studying observables related to a notion of continuous spacetime is indispensable.

One observable ideally suited for this task is the spectral dimension D_s of spacetime, since it can be calculated both for discrete and continuous spacetimes and thus straightforwardly compared in various scenarios. In a nutshell, the spectral dimension is an effective dimension as seen by a free scalar field diffusing on the spacetime. From this diffusion process one can deduce a dimension, which in flat (continuum) spacetime agrees with the topological dimension D. Interestingly, this effective dimension can change depending on the length scale at which spacetime is probed.

In many approaches to quantum gravity such a behavior has been observed, strikingly in a similar way [5]: a flow of the spectral dimension to a value smaller than $D = 4$ occurs at short length scales [6–17]. Crane and Smolin studied the distribution of virtual black holes and found a dimensional reduction at short scales depending on the distribution [6,7]. In causal dynamical triangulations (CDT) [18] a dimensional flow from $D_s = 4$ to $D_s = 2$ is found at short scales in a phase resembling a de Sitter spacetime (though more recent CDT calculations [10] rather hint at $D_s \simeq 3/2$). Modified dispersion relations effect a similar dimension flow in the asymptotic safety scenario [11], Horava-Lifshitz gravity [12] or noncommutative field theory [13–15]. In causal set theory [19], a causal spectral dimension [20] is defined essentially taking into account the causal structure fundamental to a causal set and a dimensional reduction is found at short scales [21]. Also in loop quantum gravity there exist indications for a dimensional flow, either in

*ssteinhaus@perimeterinstitute.ca
†johannes.thuerigen@physik.hu-berlin.de

terms of the scaling of the area spectrum [16] or due to a particular superposition of spin network states [22]. Naturally the question arises whether this behavior is a universal feature of quantum gravity [5] and what observational consequences might exist [23].

Explicit evaluation of physically relevant observables like the spectral dimension remains one of the most pressing issues in the spin-foam approach to quantum gravity [24]. The idea of spin-foam models is to give a rigorous definition of the quantum-gravity path integral based on the first-order formalism for general relativity as a constrained topological BF theory [25,26]. There are various proposals on how to implement these constraints on the quantum level [27–33]. While they can be justified by giving the right semiclassical limit to the amplitudes of Regge calculus locally [34], it remains an open issue to understand and control the quantum dynamics of extended spacetimes. The dependence of the spin-foam amplitude on a given cell complex can be removed either by a summation rule as provided by group field theory [35–38] or by a renormalization procedure based on coarse graining [39–42]. Only then is it possible to define the quantum expectation value of observables.

In this work we attack the challenge to compute the spectral dimension in spin-foam models, more precisely in the well-studied Engle-Pereira-Rovelli-Livine and Freidel-Krasnov (EPRL-FK) model for four-dimensional Euclidean gravity. Studying the spectral dimension for this model in full generality is currently out of reach due to the complexity of spin-foam models in general. Thus we restrict ourselves to a subset of the full gravitational path integral, so-called quantum cuboids [43–45]. This model encodes two major approximations. The first is a restriction of the combinatorics to hypercubic lattices. Note that this does not restrict the *geometry* to a hypercubic lattice as it is encoded not in the 2-complex but the group theoretic data. In a second step we furthermore restrict these data to be of hypercuboid form by restricting the path integral to specific coherent Livine-Speziale intertwiners [46] that are of cuboid form. Analogous to the calculations for the 4-simplex, the spin-foam amplitude was calculated using a stationary phase approximation, often called the large-j limit, in [43] resulting in a rational function of irreducible representations of SU(2). The associated Regge action evaluated on the stationary and critical points vanishes, which implies that the internally flat hypercuboids are glued together in a flat way resulting in flat discrete spacetime. Thus, quantum cuboids represent a superposition of flat discrete geometries of different shapes and sizes.

Despite its simplicity this model revealed a few interesting properties. An Abelian subgroup of diffeomorphisms which corresponds to moving an entire hyperplane of the cuboid lattice merely changes the subdivision of flat spacetime into flat building blocks [43]. However cuboid spin foams are not invariant under this transformation; yet for a specific choice of parameters this symmetry is almost realized. Furthermore the renormalization of cuboid spin foams [44,47] has been studied in detail following the refinement approach via embedding maps [39,40,48]. Remarkably indications for a phase transition and a UV-attractive fixed point were found for the single parameter of the model in a similar regime as for the displacement symmetry. As we see later on this regime is relevant for the spectral dimension as well.

In this article we study the spectral dimension of such quantum cuboids, first numerically and then extending the results analytically. In order to perform the numerical simulations efficiently while avoiding artifacts coming from compactness of the studied lattice, we consider $\mathcal{N}$-periodic spin foams, i.e. spin foams whose labels repeat themselves after $\mathcal{N}$ steps in any of the four (combinatorial) directions. We calculate the spectrum of the Laplace operator via Fourier transform on an infinite spin foam, prescribed by finitely many variables. Still, the numerical investigation is costly and cannot be extended to arbitrary large periodicities $\mathcal{N}$. For any finite $\mathcal{N}$ we find a regime (in between the minimal and maximal cutoffs) in which D_s changes continuously and can take any value between 0 and 4 (for specific values of the parameter).

Using a conjecture on the Laplace operator inspired by [49] we derive a general law for the spectral dimension depending on the periodicity $\mathcal{N}$, which is in good agreement with our numerical results. Given this relation we perform the $\mathcal{N} \to \infty$ limit and find a discontinuous phase transition between two phases, one given by spectral dimension $D_s = 0$ and $D_s = 4$, where the point of the phase transition is given by the scale-invariant spin-foam amplitude.[1] In this sense we observe the emergence of four-dimensional spacetime. At the same time the scale-invariant amplitude hints at a potential restoration of (an Abelian subgroup of) diffeomorphism invariance, where the parameter is again in a similar regime as the UV-attractive fixed point found in the renormalization group flow.

This article is organized as follows: we describe the basic setup of our calculations in Sec. II introducing the quantum cuboids, the spectral dimension, the setup of periodic spin foams and briefly discuss the numerical methods used. In Sec. II B we present the numerical results for various periodicities and provide an analytical explanation for the results derived from a conjecture of the Laplace operator. Section IV A deals with the $\mathcal{N} \to \infty$ limit showing the discontinuous phase transition in D_s and we furthermore discuss the possibility of using the spectral dimension as a condition to define a renormalization group flow. We conclude in Sec. V and give a brief outlook on which models to study in the future and which qualitative features we expect to carry over.

[1]By scale-invariant we here mean invariant under uniform scaling of all spins; i.e. the shape of the cuboid remains the same.

II. CUBOID SPIN FOAMS AND THE SPECTRAL DIMENSION

In this section we provide the definition of the spectral dimension as a spin-foam observable. We recall the general notion of spectral dimension and discuss how it can be understood as an observable in a path integral for quantum gravity. We explain how this is defined in spin-foam gravity and derive an explicit formula in the restricted case of cuboid spin-foam dynamics. Finally we illustrate how we address such dynamics using $\mathcal{N}$-periodic configurations and explain the use of numerical methods.

A. Cuboid spin-foam dynamics

Spin-foam models provide a definition of the quantum-gravity path integral. Here we give a concise outline of the ideas underlying the spin-foam approach to quantum gravity and the particular restriction we use in this work.

Spin foams are defined on discrete spacetime, more precisely the 2-skeleton Γ of a four-dimensional combinatorial (pseudo) manifold, which is a collection of V vertices v, E edges e and F faces f. This 2-complex is labeled by data from a Lie group G: Irreducible representations j_f on the faces and intertwiners ι_e on the edges, i.e. elements in the invariant subspace of the tensor product of representations meeting at this edge. A spin-foam model defines an amplitude to a given labeled 2-complex by assigning an amplitude $\mathcal{A}_v$ to vertices, $\mathcal{A}_e$ to edges and $\mathcal{A}_f$ to faces. The partition function is then given as a sum over all these labelings,

$$Z = \sum_{\{\iota_e, j_f\}} \prod_f \mathcal{A}_f(j_f) \prod_e \mathcal{A}_e(\iota_e, \{j_f\}_{f\supset e}) \times \prod_v \mathcal{A}_v(\{\iota_e\}_{e\supset v}, \{j_f\}_{f\supset v}). \tag{1}$$

For the four-dimensional Euclidean theory, which we use in this article, the underlying symmetry group is $G = \mathrm{Spin}(4)$, while $G = \mathrm{SL}(2,\mathbb{C})$ in the Lorentzian theory. The form of the amplitudes depends on the used spin-foam model.

In this article we are working with the Euclidean EPRL-FK spin-foam model [29–31], more precisely its generalization to arbitrary 2-complexes [50]. The idea underlying its construction is identifying SU(2) representations and intertwiners with $\mathrm{Spin}(4) \simeq \mathrm{SU}(2) \times \mathrm{SU}(2)$ representations and intertwiners. The identification of irreducible representations depends on the Barbero-Immirzi parameter $\gamma_{\mathrm{BI}} \in \mathbb{R}\backslash\{0, \pm 1\}$,

$$j_f^{\pm} := \frac{1}{2}|1 \pm \gamma_{\mathrm{BI}}| j_f, \tag{2}$$

with j_f, $j_f^{\pm} \in \frac{1}{2}\mathbb{N}$. For this map to be nonempty, the parameter γ must be a rational number. For the rest of the article we choose $\gamma_{\mathrm{BI}} < 1$.

For the intertwiners, which are essential for defining the edge and vertex amplitude of the spin-foam model, we introduce the so-called EPRL map $Y_e^{\gamma_{\mathrm{BI}}}$ for each edge e of the 2-complex,

$$Y_e^{\gamma_{\mathrm{BI}}} : \mathrm{Inv}_{\mathrm{SU}(2)}(V_{j_1} \otimes \ldots \otimes V_{j_n}) \to \mathrm{Inv}_{\mathrm{SU}(2)\times\mathrm{SU}(2)}(V_{j_1^+, j_1^-} \otimes \ldots \otimes V_{j_n^+, j_n^-}). \tag{3}$$

It maps an n-valent SU(2) intertwiner, where n faces carrying representations j_f meet at the edge e, into an $\mathrm{SU}(2) \times \mathrm{SU}(2)$ intertwiner and consists of two parts. The map

$$\beta_j^{\gamma_{\mathrm{BI}}} : V_j \to V_{j^+, j^-} \tag{4}$$

is defined via the unique isometric embedding of V_j into the factor of the Clebsch-Gordan decomposition of $V_{j^+,j^-} \simeq V_{j^+} \otimes V_{j^-}$. This map is applied to all faces containing that edge. To make sure the resulting vector is in the $\mathrm{SU}(2) \times \mathrm{SU}(2)$-gauge-invariant subspace of $V_{j_1^+, j_1^-} \otimes \ldots \otimes V_{j_n^+, j_n^-}$, we project onto that subspace with the projector $\mathcal{P}$. Hence, the EPRL map is

$$Y_e^{\gamma_{\mathrm{BI}}} := \mathcal{P}(\beta_{j_1}^{\gamma_{\mathrm{BI}}} \otimes \ldots \otimes \beta_{j_n}^{\gamma_{\mathrm{BI}}}). \tag{5}$$

We now have all the necessary ingredients to define the amplitudes. The face amplitude is given as

$$\mathcal{A}_f^{(\alpha)} := ((2j_f^+ + 1)(2j_f^- + 1))^{\alpha}, \tag{6}$$

which is just the dimension of the (j_f^+, j_f^-) representation to the power α. As proposed in [43], we have introduced the additional parameter $\alpha \in \mathbb{R}$, which turns out to be crucial in our analysis of the spectral dimension. To motivate it briefly, in spin foams it is commonly chosen to be either $\alpha = \frac{1}{2}$ or $\alpha = 1$. The former assigns the dimension of the SU(2) spin j_f to a face, the latter the respective $\mathrm{SU}(2) \times \mathrm{SU}(2)$ representation. However, beyond kinematical arguments, e.g. requiring invariance under the trivial subdivision of a face, this exponent is not fixed by dynamical arguments. Its choice essentially translates into a choice of the path-integral measure and is also present in other approaches to quantum gravity, e.g. Regge calculus [51–53].

The edge amplitude is simply introduced to normalize the intertwiners,

$$\mathcal{A}_e := \frac{1}{\|Y_e^{\gamma_{\mathrm{BI}}} \iota_e\|^2}. \tag{7}$$

The vertex amplitude $\mathcal{A}_v$ is given by

$$\mathcal{A}_v := \mathrm{Tr}_v\Big(\bigotimes_{e\supset v}(Y_e^{\gamma_{\mathrm{BI}}} \iota_e)\Big), \tag{8}$$

where Tr_v denotes the vertex trace acting on the tensor product of all intertwiners ι_e meeting at the vertex v in the following way. Each face f that contains the vertex v is shared exactly by two edges meeting at v. The indices of the respective intertwiners are then contracted with one another according to the combinatorics of the 2-complex.

A spin-foam configuration has a geometric interpretation in the following way. The intertwiners ι_e describe a quantum polyhedron, a chunk of three-dimensional space dual to the edge e whose boundary areas are given by the adjacent spins j_f. The combinatorics of the 2-complex then determine how these three-dimensional chunks of space are glued together to form a four-dimensional geometry. Summing over the areas of faces and shapes of three-dimensional polyhedra then implements a discrete sum over four-dimensional geometries.

Note that the 2-complex Γ is a choice. Several possibilities have been suggested in the literature to account for the dependence on this choice. A straightforward idea is to sum over all 2-complexes of a certain class, thus capturing all possible discretizations permitting a transition between boundary states. The most systematic implementation of this idea is group field theory [36–38] where spin-foam amplitudes appear as amplitudes in the perturbative sum labeled by Feynman diagrams Γ. There the question of consistency is addressed in terms of renormalizability of the theory. Alternatively it is possible to start with a fixed 2-complex Γ, yet one has to make sure that the calculated results are consistent with choosing a finer 2-complex Γ'. To this end one has to relate amplitudes across 2-complexes guaranteeing the same physical transitions. This is done by identifying states across boundary Hilbert spaces (via so-called embedding maps) akin to the construction of the kinematical Ashtekar-Lewandoswki vacuum in loop quantum gravity [54,55].

1. Quantum cuboids

In the present work we study the spectral dimension of spin foams restricted to hypercuboid geometries [43]. We choose the combinatorial 2-complex Γ to be hypercubic in the sense that it is the 2-skeleton of (the combinatorial dual complex of) a hypercubic lattice. In general, such a choice does not imply that also the geometry is hypercubic as this is encoded by the group representation data labeling the foam. To specify hypercuboid geometries, we consider the state sum Eq. (1) not for all possible intertwiners ι_e but only for a specific one which is sharply peaked on the shape of a cuboid. We define a cuboid intertwiner ι_{j_1,j_2,j_3} as the six-valent coherent Livine-Speziale intertwiner [46]

$$|\iota_{j_1,j_2,j_3}\rangle = \int_{\mathrm{SU}(2)} dg\, g \triangleright \bigotimes_{i=1}^{3} |j_i, e_i\rangle |j_i, -e_i\rangle \qquad (9)$$

that is the group-averaged tensor product of six coherent SU(2) states peaked on the directions given by the (orthogonal) unit vectors $e_1 = \exp(-i\pi\sigma_2/4) \triangleright e_3$, $e_2 = \exp(-i\pi\sigma_1/4) \triangleright e_3$ and e_3 in $\mathbb{R}^3$. Note that the spins on opposite faces are chosen to be equal and the associated normal vectors are antiparallel. The normal vectors e_i assigned to adjacent faces are orthogonal matching the cuboid geometry (see Fig. 1). This intertwiner exists for all choices of spins j_1, j_2 and j_3 and is always nonvanishing.

The cuboid intertwiner defines the amplitudes of this restricted EPRL model. First the intertwiner is boosted by the previously introduced EPRL map Y_e^{BI}. For a Barbero-Immirzi parameter $\gamma_{\mathrm{BI}} < 1$ the vertex amplitude factorizes

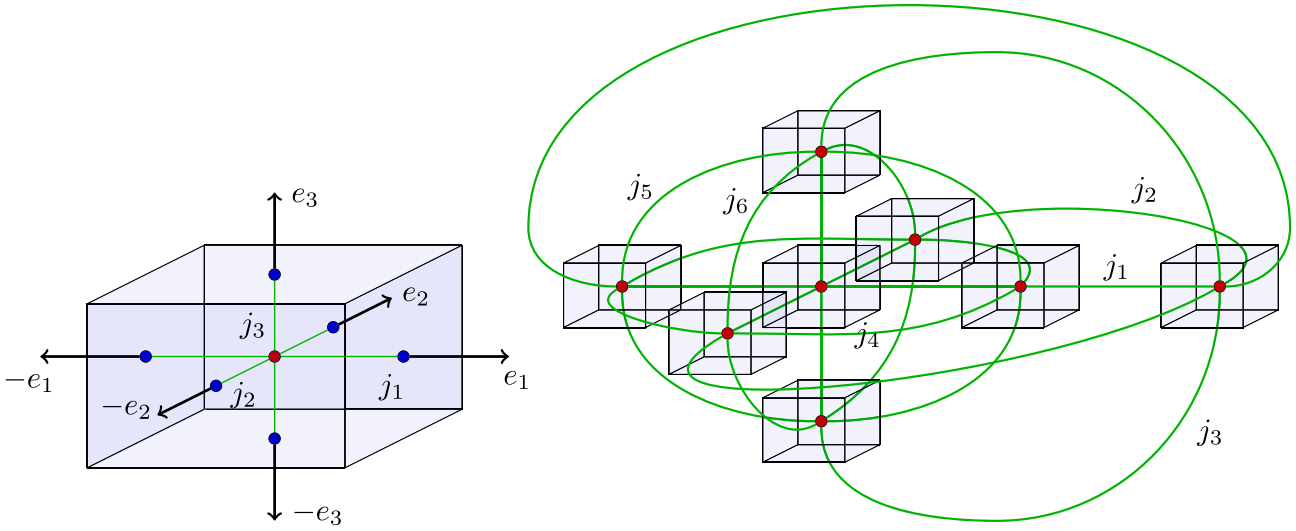

FIG. 1. Left: The six-valent cuboid intertwiner. Spins j_i on opposite edges of the vertex are the same and the corresponding unit vectors $\pm e_i$ are antiparallel. In the semiclassical limit the spins are the areas and the unit vectors the normals of the cuboid faces. Right: The spin network dual to a hypercuboid. Because of the translation invariance of spins along each cuboid's face direction in $D = 4$ there are $\binom{D}{2} = 6$ spins.

as $\mathcal{A}_v = \mathcal{A}_v^+ \mathcal{A}_v^-$; i.e. each of them only depends on the spins $\{j^+\}$ or $\{j^-\}$ respectively. These amplitudes are given by

$$\mathcal{A}_v^\pm = \int_{\mathrm{SU}(2)^8} dg_a \, e^{S^\pm[g_a]} \tag{10}$$

with the complex action

$$S^\pm[g_a] = \frac{1 \pm \gamma}{2} \sum_l 2j_l \ln\langle -\vec{n}_{ab} | g_a^{-1} g_b | \vec{n}_{ba} \rangle, \tag{11}$$

where a, b denote the intertwiners, l the (oriented) links connecting them in the vertex trace and $|\vec{n}_{ab}\rangle$ the SU(2) coherent state peaked on the directions given by $\vec{n}_{ab}$ in the fundamental representation $j = \frac{1}{2}$.

For the remainder of the article, we work in the large-j limit, usually understood as the semiclassical limit when keeping areas $A_f \sim \hbar j_f$ fixed, which was computed first for the EPRL-FK model for boundary data corresponding to a generic, nondegenerate 4-simplex [56–58]. This limit allows us to perform a stationary-phase analysis of the vertex amplitude Eq. (10) by simultaneously scaling up all spins at once. For hypercuboid intertwiners the calculation was performed in [43], and here we only review the basic steps and present the results.

The vertex amplitude $\mathcal{A}_v^\pm$ is given as an integral over eight copies of SU(2), where one integration is obsolete due to the invariance of the Haar measure. The remaining integral has several isolated critical points which are related by the 2^7-fold symmetry under changing $g_a \to -g_a$. Modulo this symmetry the two critical and stationary points satisfy the following equations for all links (ab),

$$g_a \rhd \vec{n}_{ab} = -g_b \rhd \vec{n}_{ba}. \tag{12}$$

The two distinct solutions and more details can be found in [43]. The solution reads

$$\mathcal{A}_v^\pm = \left(\frac{1 \pm \gamma_{\mathrm{BI}}}{2}\right)^{\frac{21}{2}} \mathcal{B}_v \tag{13}$$

with

$$\mathcal{B}_v(j_1, \ldots, j_6) = \frac{1}{\sqrt{\det H}} + \text{c.c.} \tag{14}$$

H denotes the matrix of second derivatives of S, and its determinant is given by

$$\det H = 2 \prod_{\substack{\{ijkl\}= \\ \{1256\},\{1346\},\{2345\}}} \left(\sum_{\{abc\} \subset \{ijkl\}} j_a j_b j_c \right) \prod_{\substack{\{ikl\}= \\ \{124\},\{135\},\{236\},\{456\}}} \left((1+\mathrm{i}) j_i j_k j_l + \sum_{\{ab\} \subset \{ikl\}} (j_a^2 j_b + j_a j_b^2) \right) \tag{15}$$

where the first product is over all but two opposite edges in a tetrahedron with edges labeled 1,2,3,4,5,6 as is a multiple subgraph in the hypercuboid spin network (Fig. 1); the second product runs over the tetrahedron's faces. Note that the action $S^\pm$ evaluated on the critical and stationary points vanishes exactly. This shows, at least in the large-j limit, that the dynamics demand the quantum cuboids to be glued together in a flat way. Furthermore we can readily see that the vertex amplitude is a purely rational function and does not contain any oscillating parts.

In a similar way one calculates the asymptotic expansion of the edge and face amplitudes. Here we simply present the results,

$$\| Y_e^{\gamma_{\mathrm{BI}}} \iota_{j_1, j_2, j_3} \| \sim \frac{8(1 - \gamma_{\mathrm{BI}}^2)^{-\frac{3}{2}}}{(j_1 + j_2)(j_1 + j_3)(j_2 + j_3)}, \tag{16}$$

and

$$\mathcal{A}_f^{(\alpha)} \sim j_f^{2\alpha}. \tag{17}$$

Combining these results, we obtain the partition function Eq. (1) in the large-j limit,

$$\begin{aligned} Z &\sim \left(\frac{1-\gamma^2}{4}\right)^{\alpha F - \frac{3}{2}E + \frac{21}{2}V} \sum_{j_f} \prod_f j_f^{2\alpha} \prod_e (j_1 + j_2)(j_2 + j_3)(j_1 + j_3) \prod_v \mathcal{B}_v^2 \\ &=: \left(\frac{1-\gamma^2}{4}\right)^{(6\alpha - 9/2)V} \sum_{j_f} \prod_v \hat{\mathcal{A}}_v^{(\alpha)}. \end{aligned} \tag{18}$$

In the last step we have combined the vertex, edge and face amplitudes into single amplitude $\hat{\mathcal{A}}_v^{(\alpha)}$ assigned to each vertex thanks to the regular combinatorics of the hypercubic lattice.

Let us briefly recall some properties of the amplitude $\hat{\mathcal{A}}_v^{(\alpha)}$. It is a homogeneous function of degree $12\alpha - 9$ in all spins,

$$\hat{\mathcal{A}}_v^{(\alpha)}(\{\lambda j_i\}) = \lambda^{12\alpha-9}\hat{\mathcal{A}}_v^{(\alpha)}(\{j_i\}). \tag{19}$$

This scaling property plays an important role later on. Furthermore, $\hat{\mathcal{A}}_v^{(\alpha)}$ depends on six SU(2) spins j_i giving the area of the faces of the hypercuboid. These are two more degrees of freedom than the four edge lengths prescribing a hypercuboid allowing for nongeometric configurations. Nongeometricity here refers to a nonmatching of shapes of faces [59], reminiscent of the twisted geometries parametrization of the loop quantum gravity phase space [60].

For hypercuboid spin foams to be purely geometric, the six spins prescribing it have to satisfy three conditions,

$$j_1 j_6 = j_2 j_5 = j_3 j_4, \tag{20}$$

which state that the 4-volume calculated from these spins is the same no matter which two faces (only sharing a vertex in the dual discretization) of the hypercuboid are chosen. Then the areas of faces can be unambiguously expressed in terms of four edge lengths. Note that if two of the above equations are satisfied the third follows automatically.[2] These conditions are closely related to volume simplicity constraints [61].

Restricting the spin-foam state sum to geometric configurations implies integrating over edge lengths instead of SU(2) spins. Besides the Jacobian picked up due to the change of variables, we have to take into account that we integrate over a submanifold of the original integration domain. The necessary Fadeev-Popov determinant taking care of the additional spins being gauge fixed is derived in detail in Appendix B of [45].

After this restriction the only configurations that are allowed are irregular lattices, yet all angles are right angles; i.e. the hypercuboids can take any shape as long as they remain hypercuboids. As a result all internal deficit angles vanish, such that these geometries are flat. Thus nontrivial effects on the spectral dimension of the quantum geometry can only stem from the way these geometries are superposed. In turn this is solely determined by the weight assigned to them by the spin-foam amplitudes, in particular, geometries of different *scale*.

[2]Each three-dimensional cuboid is prescribed by three areas, which are in 1-to-1 correspondence to three edge lengths unless one of the areas vanishes. Equation (20) ensures that these edge lengths from individual cuboids agree for all cuboids of the hypercuboid, ensuring shape matching of faces.

The function $\hat{\mathcal{A}}_v^{(\alpha)}$ as a function of edge lengths has a different scaling behavior compared to the spin case due to the restriction to purely geometric geometries (encoded in the Fadeev-Popov determinant). It is still a homogeneous function in all edge lengths, but of degree $24\alpha - 14$,

$$\hat{\mathcal{A}}_v^{(\alpha)}(\{\lambda l_i\}) = \lambda^{24\alpha-14}\hat{\mathcal{A}}_v^{(\alpha)}(\{l_i\}). \tag{21}$$

Again, this behavior becomes important in our analysis of the results below.

B. Spectral dimension and Laplacian on spin-foam geometry

The spectral dimension on a geometry is the dimension as seen by a fictitious field propagating on that geometry. The standard case is a Riemannian manifold $(\mathcal{M}, g)$ where the spectral dimension is defined as the scaling

$$D_s(\tau) := -2\frac{\partial \ln P(\tau)}{\partial \ln \tau} \tag{22}$$

of the trace

$$P(\tau) = \mathrm{Tr}_{\mathcal{M}} K(x, x_0; \tau) = \int_{\mathcal{M}} \mathrm{d}x_0 \sqrt{g} K(x_0, x_0; \tau) \tag{23}$$

of the heat kernel $K(x, x_0; \tau)$ solving

$$\partial_\tau K(x, x_0; \tau) - \Delta_x K(x, x_0; \tau) = 0 \tag{24}$$

with appropriate boundary conditions [usually $K(x, y; 0) = \delta(x - y)$]. Thus, the heat-kernel trace $P(\tau)$ depends on the geometry via the Laplacian operator Δ acting on functions, i.e. scalar fields ϕ.

We consider the spectral dimension of quantum spacetime as the scaling of the quantum expectation value of the heat-kernel trace and focus on path-integral formalism here. Conceptually, suppose there is a definition of a gravity path integral as a sum over geometries g,

$$Z = \int_{\mathcal{M}} \mathcal{D}g\, \mathrm{e}^{\mathrm{i}S_{\mathrm{GR}}[g]}. \tag{25}$$

Then, the according quantum spectral dimension should be defined in terms of the expectation value of the heat kernel as an insertion into the path integral,

$$\langle P(\tau)\rangle = \frac{1}{Z}\int_{\mathcal{M}} \mathcal{D}g\, P(\tau)\mathrm{e}^{\mathrm{i}S_{\mathrm{GR}}[g]}, \tag{26}$$

that is,

$$D_s = -2\frac{\partial \ln\langle P(\tau)\rangle}{\partial \ln \tau}. \tag{27}$$

Here we consider the precise definition of a path-integral proposal as given by the spin-foam dynamics defined in the previous section. This is a discrete path integral. Thus the

main remaining task for the definition of the quantum spectral dimension is the definition of the Laplacian in the heat equation Eq. (24) on spin-foam configurations. Then the heat kernel and its trace $P(\tau)$, the observable to be inserted in the state sum, follow as solutions to this equation.

The Laplace operator on spin configuration can be defined using a proper definition on discrete geometries. The Laplacian acting on a function ϕ defined on the dual vertices v_n of a four-dimensional combinatorial complex with attached geometry depends on the four-volumes $V^n_{(4)}$ dual to v_n, the boundary three-volumes V^{mn} between dual vertices v_n and v_m as well as the lengths $l^{mn}_\star$ of the edges dual to these three-volumes [62],

$$-(\Delta\phi)_m = -\sum_{n\sim m}\Delta_{mn}(\phi_m-\phi_n) = \frac{1}{V^m_{(4)}}\sum_{n\sim m}\frac{V^{mn}}{l^{mn}_\star}(\phi_m-\phi_n), \tag{28}$$

where $n\sim m$ indicates adjacency of the vertices v_m, v_n. There are various ways to define these volumes and dual lengths in terms of spin-foam degrees of freedom [62]. Area variables are most natural as they are directly related to the spins j labeling the configurations [63], but they might be insufficient to uniquely determine discrete geometry [64]. This issue can be overcome using flux or area-angle variables [65,66]. For the present purpose area variables given by spins are sufficient because all angles are considered as right angles in the hypercuboid restriction.

The Laplacian on cuboid spin foams can be expressed in terms of spins. A semiclassical configuration has a geometric interpretation in terms of an assignment of areas

$$A_f = \ell^2_\gamma j_f \tag{29}$$

to the squares of the hypercubic lattice (where the dimensionfull constant ℓ_γ is of the order of the Planck length and might depend further on the Barbero-Immirzi parameter γ_{BI}). Due to the form of cuboid intertwiners Eq. (9), two areas agree whenever they are parallel and one is reached from the other by a translation perpendicular to them. That is, denoting directions on the lattice $\mu,\nu,\ldots\in\{0,1,2,3\}$ and lattice sites $\vec{n}\in\mathbb{Z}^4$,

$$A^{\vec{n}+re_\rho+se_\sigma}_{\mu\nu} = A^{\vec{n}}_{\mu\nu}, \tag{30}$$

where μ, ν, ρ, σ are all different directions, e_μ are unit vectors in the μ direction, and $r,s\in\mathbb{Z}$.

Areas uniquely determine three-dimensional cuboid geometry but not four-dimensional hypercuboid geometry. A cuboid is equally determined by its three edge lengths l_1, l_2, l_3 or square areas $A_{ij}=l_il_j$ in terms of the inverse relation

$$l_i^2 = \frac{A_{ij}A_{ik}}{A_{jk}}. \tag{31}$$

A semiclassical quantum hypercuboid dual to a vertex $\vec{n}\in\Gamma$ is the four-dimensional geometry determined by the six areas $A^{\vec{n}}_{\mu\nu}$, $\mu<\nu$. It has two extra degrees of freedom compared to the four edge lengths l_μ of classical hypercuboid in $\mathbb{R}^4$. Accordingly, it is generically not geometric in the sense that using edge-area relations Eq. (31) on each cuboid face does not lead to a consistent set of edges, an instance of "twisted geometry" [60]. This is only the case if the geometricity conditions Eq. (20) are fulfilled, that is for areas

$$A_{01}A_{34} = A_{13}A_{24} = A_{14}A_{23}. \tag{32}$$

The three terms are simply the possible expressions of the 4-volume in terms of areas. One can check that if these agree, all expressions for edge lengths agree as well.

Edge lengths and 4-volumes of a semiclassical quantum hypercuboid can be defined naturally as averages over their distinct expressions in area. Thus, the generalized 4-volume of such a hypercuboid dual to $\vec{n}$ is

$$V^{\vec{n}}_{(4)} := \left(\prod\nolimits_{\mu<\nu}A^{\vec{n}}_{\mu\nu}\right)^{\frac{1}{3}}. \tag{33}$$

This allows us to define the generalized length of an edge in direction μ in this hypercuboid as

$$l^{\vec{n}}_\mu := \frac{V^{\vec{n}}_{(4)}}{(A^{\vec{n}}_{\nu\rho}A^{\vec{n}}_{\nu\sigma}A^{\vec{n}}_{\rho\sigma})^{\frac{1}{2}}} = \frac{(A^{\vec{n}}_{\mu\nu}A^{\vec{n}}_{\mu\rho}A^{\vec{n}}_{\mu\sigma})^{\frac{1}{3}}}{(A^{\vec{n}}_{\nu\rho}A^{\vec{n}}_{\nu\sigma}A^{\vec{n}}_{\rho\sigma})^{\frac{1}{6}}}. \tag{34}$$

With these definitions one has $V_{(4)}=l_0l_1l_2l_3$ even for nongeometric configurations.

Similar to the generalized 4-volume, Eq. (33), we define three-dimensional volumes for neighboring vertices $\vec{m}$ and $\vec{n}=\vec{m}+e_\mu$,

$$V^{\vec{m}\,\vec{n}} := V^{\vec{m}}_{\nu\rho\sigma} = l^{\vec{m}}_\nu l^{\vec{m}}_\rho l^{\vec{m}}_\sigma = (A^{\vec{m}}_{\nu\rho}A^{\vec{m}}_{\nu\sigma}A^{\vec{m}}_{\rho\sigma})^{\frac{1}{2}} \tag{35}$$

using that areas on the boundary between $\vec{m}$ and $\vec{n}$ match due to the translation invariance Eq. (30). Finally, a simple way to define the dual lengths $l_\star$ is in terms of a geometric mean,

$$l^{\vec{m}\,\vec{n}}_\star = \sqrt{l^{\vec{m}}_\mu l^{\vec{n}}_\mu} \overset{\text{Eq. (34)}}{=} \frac{(A^{\vec{m}}_{\mu\nu}A^{\vec{m}}_{\mu\rho}A^{\vec{m}}_{\mu\sigma})^{\frac{1}{6}}}{(A^{\vec{m}}_{\nu\rho}A^{\vec{m}}_{\nu\sigma}A^{\vec{m}}_{\rho\sigma})^{\frac{1}{12}}}\frac{(A^{\vec{n}}_{\mu\nu}A^{\vec{n}}_{\mu\rho}A^{\vec{n}}_{\mu\sigma})^{\frac{1}{6}}}{(A^{\vec{n}}_{\nu\rho}A^{\vec{n}}_{\nu\sigma}A^{\vec{n}}_{\rho\sigma})^{\frac{1}{12}}}. \tag{36}$$

With these definitions, the matrix elements of the Laplacian as functions of areas are

$$\Delta_{\vec{m}\,\vec{n}} = \frac{1}{\sqrt{A^{\vec{m}}_{\mu\nu}A^{\vec{m}}_{\mu\rho}A^{\vec{m}}_{\mu\sigma}}}\frac{(A^{\vec{n}}_{\nu\rho}A^{\vec{n}}_{\nu\sigma}A^{\vec{n}}_{\rho\sigma})^{\frac{1}{3}}}{(A^{\vec{n}}_{\mu\nu}A^{\vec{n}}_{\mu\rho}A^{\vec{n}}_{\mu\sigma})^{\frac{1}{6}}}. \tag{37}$$

With this Laplacian, the heat equation Eq. (24) becomes a difference equation solved by the heat kernel $K(\vec{n},\vec{m};\tau)$ on the semiclassical spin-foam configuration. Its trace analogous to Eq. (23) is simply the sum over vertices in the 2-complex Γ [62,67],

$$P(\tau) = \mathrm{Tr}K(\vec{n},\vec{m};\tau) = \sum_{\vec{n}\in\Gamma} K(\vec{n},\vec{n};\tau). \tag{38}$$

This completes the definition of the spectral dimension on a single semiclassical spin-foam configuration as the scaling Eq. (27) of $P(\tau)$. Inserting this expression in the spin-foam state sum yields corresponding quantum expectation value.

While the given definitions of semiclassical geometry entering the Laplacian, though natural, might allow also for alternatives, results on the spectral dimension of discrete geometries [67,68] suggest that it is not sensitive to details of the precise definition of local geometry. For example, from the perspective of discrete geometry of the dual complex, a dual-length definition in terms of the arithmetic mean $l^{\vec{m}\,\vec{n}}_{\star} = (l^{\vec{m}}_{\mu} + l^{\vec{n}}_{\mu})/2$ might be more appropriate [62]. While the resulting expression for Laplacian coefficients $\Delta_{\vec{m}\,\vec{n}}$ is slightly more involved, this is irrelevant for all practical purposes. In particular, we have cross-checked that the calculations presented in this paper with either definition show no significant differences.

C. Approaching the full dynamics in terms of periodic configurations

Evaluating the quantum spectral dimension remains an intriguing challenge even after restricting the spin-foam path integral to the asymptotic regime of quantum cuboids Eq. (18). This challenge is posed by both ingredients of the calculation, the spectral dimension and computing the spin-foam state sum. To clarify this point, let us disentangle the two and discuss first the evaluation of the spectral dimension of one lattice.

Consider a discrete geometry, for simplicity with periodic boundary conditions, i.e. a D-dimensional torus, on which the discrete Laplace operator Eq. (28) is well defined. Its spectral dimension can be reliably determined in a certain regime of the diffusion time τ, namely $a \ll \sqrt{\tau} \ll aN_{\mathrm{lattice}}$. Here a denotes the lattice scale and N_{lattice} is the number of lattice sites in each direction.[3] If τ is smaller or similar to the lattice scale a, the return probability remains constant or only changes slightly as we cannot resolve the geometry below the lattice scale, resulting in a spectral dimension $D_s = 0$. Seen by a random walker the diffusion time is too small for the random walker to explore the surrounding geometry or for it to even leave the initial lattice site. Conversely when τ goes beyond the size N_{lattice} of the lattice the return probability becomes constant again due to the compactness of the geometry, and thus $D_s = 0$. Again for a random walker the diffusion time was long enough for the walker to travel through the entire geometry to arrive back at the starting point. Hence in order to observe a nontrivial spectral dimension the lattice size must be large enough, which is determined by the number of lattice sites in each direction. Typically N_{lattice} should be at least of the order $\sim 10^3$. However it might be necessary that the number of lattice sites is a few orders of magnitude larger than this such that the compactness is not seen too early. An example could be a 2-torus with a small and a large radius: If the lattice scale is too large, one cannot resolve the small radius.

Given such a lattice, for concreteness in $D = 4$, it is numerically challenging to compute the spectral dimension. In order to derive the return probability at all scales τ, in particular at the intermediate ones between the lattice and compactness scale, we have to know the *entire* spectrum of the Laplace operator Δ. For $N_{\mathrm{lattice}} \sim 10^3$ in each direction, Δ is a $10^{12} \times 10^{12}$ matrix that needs to be diagonalized. Already memory cost in defining such a matrix is very high, not to mention the computational cost in computing its complete spectrum.[4]

Instead of diagonalizing the entire matrix one can study the return probability of a discrete geometry via a random walker, similar to the studies in causal dynamical triangulations [18]. The random walker randomly jumps from lattice site to lattice site, where the jump probabilities are related to the entries of Δ. The return probability literally is the probability of the random walker to return to the lattice site it started from after σ steps, where σ can be related to the diffusion scale τ. This probability is then averaged over each lattice site as a possible starting point of the random walker. Particular care must be given to the implementation of the algorithm as soon as cells can vary in their respective volume, which we detail in a companion article. In order to correctly estimate the return probability a random walk must be frequently repeated. While it is very efficient in memory consumption and thus can be straightforwardly implemented, the number of possible paths grows exponentially requiring a similarly growing number of repetitions to allow for accurate results. Hence the computational cost grows quickly when large lattice distances are considered. Since each random walk is independent of the others, this process is straightforwardly parallelizable.

Conversely the formal requirements to accurately calculate the spectral dimension pose a serious challenge to the spin-foam approach. So far most studies of spin-foam

[3]For simplicity we assume the lattice to be of equal size in all dimensional directions.

[4]Since Δ is proportional to the adjacency matrix many of its entries are empty. Thus one might be tempted to work with sparse matrices instead. However, algorithms computing eigenvalues of sparse matrices are only efficient for a small number of eigenvalues, usually its largest or smallest. Such an approach is hence only feasible when studying small or large scales respectively.

models did not exceed a few spin-foam vertices; in fact most calculations were actually performed for a single 4-simplex in the so-called large-j limit. Going beyond this asymptotic expansion has recently been explored in [59], see also [69] concerning the Barrett-Crane spin-foam model [27,28], but it has not yet been used to study the spin-foam partition function for discretizations consisting of several building blocks. One of the authors studied the restricted partition function of hypercubic spin foams for slightly larger discretizations in the large-j limit in [44,45]. However at the current stage studying the spectral dimension of spin foams in full generality is out of reach.

To make matters worse, a dynamical quantum geometry might require even larger lattice if one intends to study the quantum spectral dimension. Without imposing restrictions onto the spin-foam state sum, we superimpose geometries of varying size since we are summing over spins, which can range over many orders of magnitude.[5] Hence it is straightforward to conceive a scenario where we superimpose a small and a comparatively large geometry. In a foam with a fixed number of vertices this can result in a situation where we run into the compactness scale of the small geometry, which can result in a biased result.

Naturally the question arises how we can reconcile the need of studying small lattice in order to keep the spin-foam state sum tractable with the imperative to make the lattice as large as possible (if not infinite) in order to reliably compute the spectral dimension. To kill two birds with one stone we introduce $\mathcal{N}$-periodic lattice; i.e. we introduce an internal $\mathcal{N}$ periodicity to the lattice: after $\mathcal{N}$ steps the geometric labels of the foam are the same, in any of the four dimensions. On the one hand this greatly simplifies the calculation of the spectrum of the Laplacian: instead of diagonalizing a matrix of the size of the entire lattice we perform a Fourier transform and calculate the spectrum of the Brillouin zone from a $\mathcal{N}^D \times \mathcal{N}^D$ matrix. The total lattice size then merely determines which discrete frequencies of this spectrum are allowed. In the limit of an infinite lattice we simply integrate over the entire spectrum when calculating the return probability.

On the other hand, the spin-foam state sum gets drastically simplified, since the dynamical variables have to respect the $\mathcal{N}$ periodicity. Hence the summation is only over the variables associated to an "$\mathcal{N}$-cell." This $\mathcal{N}$-cell then determines the geometry of the entire lattice, where the configuration of this cell is weighted by the spin-foam amplitudes of the entire lattice. Increasing the total lattice site implies weighing the configuration with a higher power of spin-foam amplitudes. The latter fact makes numerical simulations increasingly difficult and thus obstructs us from taking the limit of large lattices, such that we have to introduce an additional approximation: We assume the $\mathcal{N}$-cell to be weighted only by the spin-foam amplitudes associated with that $\mathcal{N}$-cell. Let us justify this approximation:

As we have discussed above the $\mathcal{N}$ periodicity greatly simplifies our calculation: the *entire* spectrum is readily available and the spin-foam state sum is much more tractable. The choice to take the infinite lattice limit is solely introduced to avoid the compactness scale of some quantum geometries and does not qualitatively affect the spectrum otherwise. Furthermore increasing the power of the spin-foam amplitudes changes the behavior only slightly, which we discuss below in more detail. The crucial limit indispensable for computing the spectral dimension is taking $\mathcal{N} \to \infty$. Using a conjecture about the scaling behavior of Δ inspired by [49] and in agreement with our numerical results, we calculate that limit.

Calculating the return probability for $\mathcal{N}$-periodic hypercubic spin foams (in the large-j limit) boils down to performing several integrations: on the one hand we have to integrate over spin-foam labels, i.e. SU(2) spins, on the other hand over the eigenvalues of the Laplacian operator, here captured in branches of frequencies. The number of spins to integrate over increases with growing $\mathcal{N}$, while the number of integrations over eigenvalues remains 4 for four spacetime dimensions.

We perform the numerical integrations in `Julia`[6] using the `Cuba`[7] package [70], a set of adaptive algorithms using Monte Carlo techniques suited for higher dimensional integration. Instead of performing all integrations at once, we integrate over the eigenvalues of the Laplacian first. Hence the separate integrations are lower dimensional improving convergence of the algorithms.

III. DIMENSIONAL FLOW IN SPIN FOAMS

Before we present our results on the spectral dimension of hypercuboid spin foams, in particular how it changes with the scale at which the geometry is probed, we would like to briefly recall the key geometric properties of these configurations.

In the large-j limit hypercuboid spin foams are essentially peaked on flat building blocks that are glued together in a flat way. The spins solely determine the size of faces, the 3-volume of cuboids and the 4-volume of hypercuboids. Thus they affect the entries of the Laplacian, but spacetime in itself remains flat.

The main effect on the spectral dimension comes from the superposition of geometries of different size, more concretely how geometries of different size are weighted in the path integral depending on the parameter α. Indeed this determines which spectral dimension we observe. We first present the results for geometric configurations where each

[5]Whether this actually is the case and which geometries are preferred depends crucially on the spin-foam amplitudes.

[6]https://julialang.org/.

[7]See http://www.feynarts.de/cuba/ for the original version and https://github.com/giordano/Cuba.jl for the `Julia` package.

hypercuboid is given by four edge lengths before briefly discussing the spin case. For all numerical simulations we have chosen the same minimal and maximal cutoff to make the results comparable. For length variables we choose $l_{\min} = 10^{-3}$ and $l_{\max} = 10^{3}$; for spins it is $j_{\min} = 10^{-6}$ and $j_{\max} = 10^{6}$ accordingly. We observe qualitatively similar results for various values of periodicity $\mathcal{N}$ justifying the finite-$\mathcal{N}$ computations.

A. Restriction to geometric configurations

1. 1-periodic configurations

The simplest example we can study is the 1-periodic case: the entire geometry is determined by a single hypercuboid and its four edge lengths l_i. Computing the return probability in this case is rather simple, since the spectrum of the four-dimensional Laplace operator can be computed from the spectra of four one-dimensional Laplace operators (for equilateral one-dimensional lattices) with edge lengths l_i. This is straightforward to recognize from Eq. (28) as the components of the four-dimensional Laplace operator in one direction only depend on the length associated with that direction; the dependence on the other lengths in the 3- and 4-volume cancels, since all angles are right angles. Thus the one-dimensional spectra associated to each of the four dimensions are

$$\omega_i^2(l_i, k_i) = \frac{2}{l_i^2}(1 - \cos(k_i)), \qquad k_i \in (-\pi, \pi]. \tag{39}$$

The full four-dimensional spectrum is the sum of one-dimensional spectra in each direction such that the heat trace factorizes and is solved analytically [67],

$$P(\tau; \{l_i\}) = \prod_{j=1}^{4}\left(\int_{-\pi}^{\pi} \mathrm{d}k_j \, \exp\left(-\frac{2\tau}{l_j^2}(1 - \cos(k_j))\right)\right) = \prod_{j=1}^{4}\left(2\pi \mathrm{e}^{-\frac{2\tau}{l_j^2}} I_0\left(\frac{2\tau}{l_j^2}\right)\right) \tag{40}$$

where I_0 denotes the modified Bessel function of first kind.

While the heat trace takes this simple product form, the amplitude $\hat{\mathcal{A}}_v^{(\alpha)}$ does not factorize into a product of amplitudes associated to a single dimension. Hence the integration over length variables must be performed simultaneously,

$$\langle P(\tau)\rangle_\alpha = \frac{1}{Z}\int \prod_{i=1}^{4} \mathrm{d}l_i \, \hat{\mathcal{A}}_v^{(\alpha)}(\{l_i\}) P(\tau; \{l_i\}) = \frac{1}{Z}\int \prod_{i=1}^{4} \mathrm{d}l_i \, \hat{\mathcal{A}}_v^{(\alpha)}(\{l_i\}) \prod_{j=1}^{4}\left(2\pi \mathrm{e}^{-\frac{2\tau}{l_j^2}} I_0\left(\frac{2\tau}{l_j^2}\right)\right). \tag{41}$$

We perform the remaining integral over lengths numerically. The spectral dimension $D_s(\tau) = D_s(\tau, \alpha)$ is again defined as the logarithmic derivative,

$$D_s(\tau) = -2\frac{\partial \ln\langle P(\tau)\rangle_\alpha}{\partial \ln \tau}. \tag{42}$$

In Fig. 2 we plot respectively the return probability and the spectral dimension as a function of τ over several orders of magnitude for different values of α. Table I contains the results (with error estimates) from finding the best linear fit for $\ln\langle P(\tau)\rangle_\alpha$ for the middle plateau. Let us describe some general features of the results.

For $\tau \ll l_{\min}^2$, we only find $D_s = 0$ as we are probing spacetime below (the smallest allowed) lattice scale. Seen from a random walker, this just means that the random walker was not able to leave the starting 4-cell at all and is thus unable to probe spacetime; hence the return probability

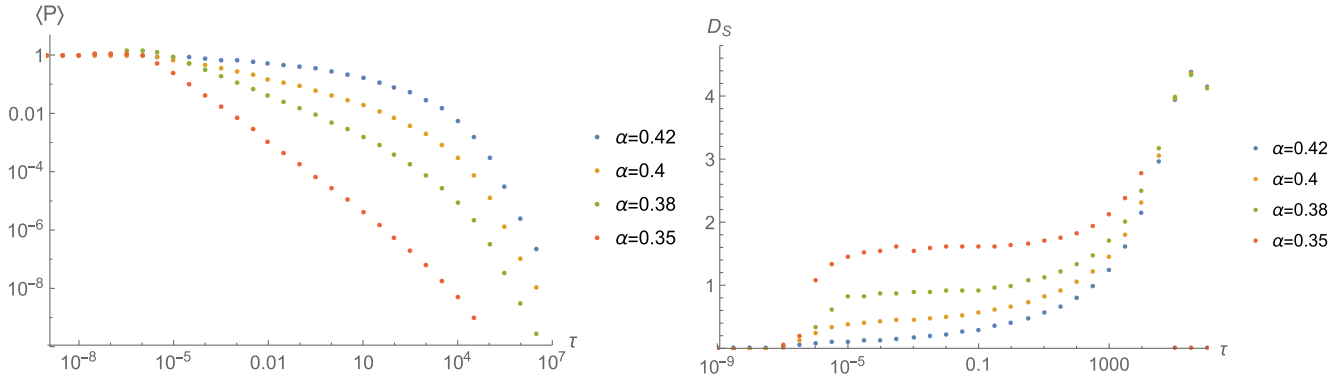

FIG. 2. Numerical results of $\langle P(\tau)\rangle$ (left) and D_s (right) for periodicity $\mathcal{N} = 1$ for various values of α. The individual points of D_s are calculated by taking the difference quotient of $\langle P(\tau)\rangle$.

TABLE I. Values of spectral dimension D_s in the 1-periodic case for the plateau $l^2_{\min} < \tau < l^2_{\max}$ obtained from a linear fit to $\langle P(\tau)\rangle_\alpha$.

α	0.42	0.4	0.38	0.35
D_s	0.	0.50 ± 0.02	0.97 ± 0.02	1.64 ± 0.02

is constantly 1. For $\tau \gg l^2_{\max}$, we always find $D_s = 4$. This is straightforward to explain as well because we are probing a superposition of four-dimensional lattices at a scale where *all* these geometries possess $D_s = 4$. As we do not add any geometries of larger lattice scale, we can only find $D_s = 4$ if we increase τ further. Thus we omit results for $\tau > 10^6$.

The behavior of D_s for $l^2_{\min} < \tau < l^2_{\max}$ depends crucially on α; namely there is an interval $[\alpha_{\min}, \alpha_{\max}]$ in which D_s changes continuously from $D_s = 4$ at $\alpha_{\min}$ and $D_s = 0$ at $\alpha_{\max}$. Outside this interval $D_s = 0$ for $\alpha > \alpha_{\max}$ and $D_s = 4$ for $\alpha < \alpha_{\min}$. It is difficult to find $\alpha_{\min}$ and $\alpha_{\max}$ numerically; below we provide an analytical derivation for these parameters, which also estimates them remarkably well in more complicated cases. We comment on the implications of this result later on.

A brief note on the cutoffs is in order: if we remove the minimal cutoff, we do not observe a drop to $D_s = 0$ to small scales unless $\alpha > \alpha_{\max}$. Instead the plateau we observe extends to smallest scales. Similarly if we remove the maximal cutoff we do not observe an increase to $D_s = 4$ for large τ unless $\alpha < \alpha_{\min}$.

2. 2-periodic configurations

The next logical step is to study a 2-periodic spin foam, that is a spin-foam completely prescribed by a block of 16 spin-foam vertices glued together. In the geometric case that we are studying here, each vertex amplitude depends on four edge lengths which are identified across the amplitudes via the gluing. As one would expect, the block of 16 vertex amplitudes then depends on eight edge lengths in total, two associated to each dimension. The scaling properties of each individual vertex amplitude are the same as before, such that the entire amplitude $\mathcal{A}$ scales according to Eq. (21) as follows (under uniform scaling of all edge lengths),

$$\mathcal{A}^{(\alpha)}_{\mathcal{N}=2} \propto \prod_v \hat{\mathcal{A}}^{(\alpha)}_v(\{\lambda l_i\}) = \lambda^{16(24\alpha-14)} \prod_v \hat{\mathcal{A}}^{(\alpha)}_v(\{l_i\}). \quad (43)$$

The Laplace operator is slightly more intricate than in the 1-periodic case, but crucially it still possesses the "factorization" property across dimensions. To see this let us consider one of its nonzero components in the x-direction,

$$-\Delta_{x,x+1} = \frac{1}{V^{(4)}} \frac{V^{(3)}}{l^*_x} = \frac{1}{l^{(1)}_x l^{(1)}_y l^{(1)}_z l^{(1)}_t} \frac{l^{(1)}_y l^{(1)}_z l^{(1)}_t}{\frac{1}{2}(l^{(1)}_x + l^{(2)}_x)} = \frac{2}{l^{(1)}_x (l^{(1)}_x + l^{(2)}_x)}. \quad (44)$$

As in the previous cases, the components of the Laplace operator in one direction only depend on the edge lengths in that particular direction. For the geometric cuboid configurations this generalizes to arbitrary periodicity $\mathcal{N}$. So, the spectrum of the Laplace operator can be computed again via computing the spectra for four one-dimensional lattices of periodicity $\mathcal{N}$, which consist of $\mathcal{N}$ eigenvalues.

The Laplace operator of a 2-periodic one-dimensional lattice comes with two off-diagonal entries, here (for example in the x-direction)

$$w_1 = \frac{2}{l^{(1)}_x (l^{(1)}_x + l^{(2)}_x)} \quad \text{and} \quad w_2 = \frac{2}{l^{(2)}_x (l^{(2)}_x + l^{(1)}_x)}. \quad (45)$$

This can be seen by swapping $l^{(1)}$ for $l^{(2)}$ in Eq. (44). The spectrum is then derived by Fourier transform exploiting the periodicity of the lattice,

$$\omega^2_\pm(k) = w_1 + w_2 \pm \sqrt{w_1^2 + w_2^2 + 2 w_1 w_2 \cos(k)}, \quad k \in (-\pi, \pi]. \quad (46)$$

Due to the 2 periodicity the spectrum has two branches. The branch ω_- goes to 0 for $k \to 0$.

Having defined all necessary ingredients we compute $\langle P(\tau)\rangle_\alpha$ in the 2-periodic case,

$$\langle P(\tau)\rangle_\alpha = \frac{1}{Z} \int \prod_{i=1}^{8} \mathrm{d}l_i \, \mathcal{A}^{(\alpha)}_{\mathcal{N}=2}(\{l_i\}) \times \prod_{j=1}^{4} \left(\sum_{s\in\{+,-\}} \int \mathrm{d}k_j \, \exp\left(-\tau \omega_s(k_j)\right) \right). \quad (47)$$

Analogous to the 1-periodic case we find the same qualitative features, in particular, an interval in α for which we can produce any value of D_s in [0, 4]. We present the numerical results in Fig. 3 and Table II.

While the qualitative features are the same, we observe a change in the α-dependence of the spectral dimension. First, the interesting interval in α has shifted towards larger values in α. Second, the size of the interval is considerably smaller compared to the 1-periodic case. Both effects can be explained by the fact that in the 2-periodic case the geometry is weighted by 16 vertex amplitudes, which results in a more "spiked" scaling behavior Eq. (43) compared to Eq. (21) in the 1-periodic case. Since the occurrence of a spectral dimension $0 < D_s < 4$ crucially depends on the superposition of discrete geometries, the suitable range of α shrinks. Furthermore this changed scaling behavior also pushes the interval to larger α.

3. 3-periodic case

We conclude the numerical study of geometric quantum cuboids with the 3-periodic case. This case is fairly

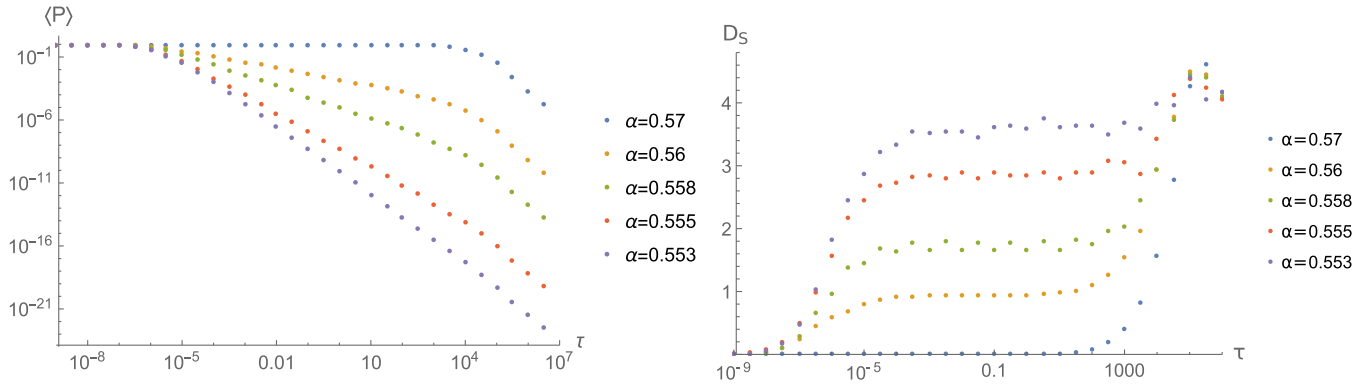

FIG. 3. Numerical results of $\langle P(\tau)\rangle$ (left) and D_s (right) in the 2-periodic case for several values of α.

analogous to the 2-periodic case, but it is already considerably more costly in computational costs.

The spin foam is determined by 81 spin-foam vertices, whose geometry is prescribed by 12 edge lengths. The scaling of this collection of amplitudes changes accordingly. The spectrum of the Laplace operator is still computed from four one-dimensional spectra, which we compute again via a Fourier transform. Its characteristic polynomial has three solutions $\omega_a^2(k_j)$, i.e. three branches.[8] Thus the return probability is computed as follows:

$$\langle P(\tau)\rangle_\alpha = \frac{1}{Z}\int \prod_{i=1}^{12} \mathrm{d}l_i\, \mathcal{A}^{(\alpha)}_{\mathcal{N}=3}(\{l_i\}) \times \prod_{j=1}^{4}\left(\sum_{a=0}^{2}\int \mathrm{d}k_j\, \exp\left(-\tau\omega_a(k_j)\right)\right). \quad (48)$$

The numerical results are presented in Fig. 4 and Table III. They confirm the observations from the 1- and 2-periodic cases: Under increasing the α-interval in which D_s changes continuously (for the plateau $l^2_{\mathrm{min}} < \tau < l^2_{\mathrm{max}}$) between 0 and 4 gets significantly smaller and it is moved to larger values of α. However the shift of the interval in α from 2 to 3 periodic is significantly smaller than from 1 to 2 periodic. This indicates that the α interval might shrink and converge to a specific value in the $\mathcal{N}\to\infty$ limit, which we discuss later on.

Since the results only change quantitatively under increasing the periodicity $\mathcal{N}$ we do not expect qualitative changes. For this reason and the growing computational costs, we refrain from studying periodicities $\mathcal{N} > 3$ numerically. Later we give an analytical argument that this is indeed not necessary. Before that we briefly study the spectral dimension in the spin case.

B. Spectral dimension of spin configurations

The restriction to purely geometric configurations is a strong simplification of spin foams. Indeed it is an intriguing question whether the nongeometric configurations can leave an imprint on the qualitative behavior of the spectral dimension. At this point we remind the reader that it is natural to expect a quantitative difference since the scaling behavior of spin configurations Eq. (19) differs from the one of geometric configurations Eq. (21).

As for the geometric case, we start our analysis with the 1-periodic case. This is prescribed by a single hypercuboid given by six spins. Not surprisingly, the spectrum of the Laplace operator for spin configurations cannot generically be expressed any more by the spectra of one-dimensional Laplace operators, since the variables and weights do not factorize any more per dimension. Fortunately, due to the 1 periodicity of the configuration, the components of the Laplacian remain unchanged under translations in any direction. Hence we compute the spectrum of the four-dimensional Laplace operator yet again from the spectra of four one-dimensional operators with spin dependent weights; e.g. in t-direction,

[8]For $\mathcal{N}\geq 3$ the off-diagonal Laplacian entries w_{ij}/V_i consist of a symmetric part $w_{ij} = V_{ij}/l^\star_{ij}$ with 3-volumes V_{ij} and dual length $l^\star_{ij}$ and the inverse 4-volume V_i (note that this Laplacian matrix is still symmetrizable [62]). For $\mathcal{N}=3$ the spectrum $x = \omega_a^2(k)$ is then given by the three real solutions to the cubic equation

$$0 = x^3 + \left(\frac{w_{12}+w_{13}}{V_1}+\frac{w_{12}+w_{23}}{V_2}+\frac{w_{13}+w_{23}}{V_3}\right)x^2 + \frac{V_1+V_2+V_3}{V_1V_2V_3}(w_{12}w_{13}+w_{12}w_{23}+w_{13}w_{23})x + 2\frac{w_{12}+w_{13}+w_{23}}{V_1V_2V_3}(1-\cos(k)).$$

TABLE II. Values for the spectral dimension D_s in the 2-periodic case for the plateau $l^2_{\mathrm{min}} < \tau < l^2_{\mathrm{max}}$.

α	0.57	0.56	0.558	0.555	0.553
D_s	0.	0.928 ± 0.011	1.74 ± 0.02	2.85 ± 0.02	3.57 ± 0.02

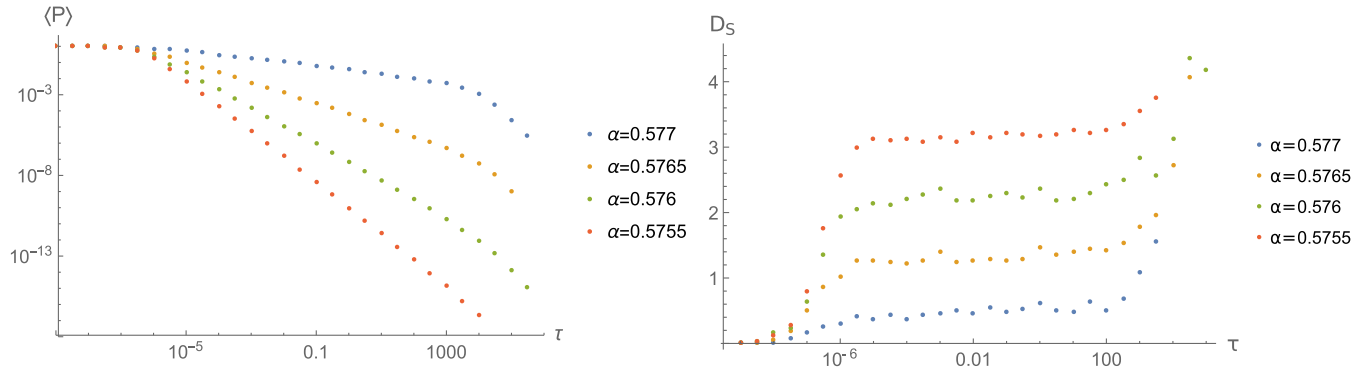

FIG. 4. Numerical results of $\langle P(\tau)\rangle$ (left) and D_s (right) in the 3-periodic case for several values of α.

$$\omega_t^2(\{j_m\}, k_t) = \frac{2}{\ell_\gamma^2}\frac{(j_1 j_2 j_3)^{\frac{1}{3}}}{(j_4 j_5 j_6)^{\frac{2}{3}}}(1-\cos(k_t)), \quad k_t \in (-\pi, \pi], \tag{49}$$

where j_4, j_5 and j_6 also span the t-direction, whereas j_1, j_2 and j_3 are purely spatial. Thus the calculation of the return probability is analogous to the geometric case, but with a slightly more intricate dependence of the spectrum on the geometry,

$$\langle P(\tau)\rangle_\alpha = \frac{1}{Z}\int \prod_{i=1}^{6} \mathrm{d}j_i\, \hat{\mathcal{A}}_v^{(\alpha)}(\{j_i\}) \times \prod_{m=1}^{4}\left(\int \mathrm{d}k_m\, \exp\left(-\tau\omega_m^2(\{j_i\}, k_m)\right)\right). \tag{50}$$

We summarize the results in Fig. 5 and Table IV.

Qualitatively we observe a similar behavior to the geometric case: For $\tau < j_{\min}$ we only find $D_s = 0$ while for $\tau > j_{\max}$ we observe only $D_s = 4$. For diffusion times τ in between we again observe that there exists an interval $[\alpha_{\min}, \alpha_{\max}]$ in which we find plateaus constant in D_s, whose value continuously increases as α is decreased. That is, $D_s = 0$ for $\alpha > \alpha_{\max}$ whereas $D_s = 4$ for $\alpha < \alpha_{\min}$. Hence we only observe a quantitative difference to the geometric case, since this α-interval is found for significantly smaller α. However the inclusion of nongeometric configurations does not seem to leave an imprint on the spectral dimension, at least not in the 1-periodic case.

For periodicity $\mathcal{N} > 1$ the spectrum of the Laplace operator does not split in directions. Thus, it is necessary to consider the entire four-dimensional operator. It is still most convenient to exploit the periodicity of the system and compute its spectrum after a Fourier transform; e.g. for $\mathcal{N} = 2$ this amounts to calculating all eigenvalues as functions of 24 spins and four momenta. Deriving these formulas analytically in full generality is challenging, not to mention for larger periodicity, but computing the spectrum numerically for fixed values of spins and momenta is efficient. Hence we can in principle continue studying the spectral dimension for larger periodicity; however the numerical cost is high. One reason is the fact that we have to perform the momentum integrations all at once instead of one by one. Moreover, already for $\mathcal{N} = 2$ we have to integrate over 24 spins, which is very costly. Thus we leave this question for future research. Nevertheless, due to the qualitative similarity of the nongeometric results to the geometric ones and the robustness of the latter for larger periodicity, we do not expect vastly different results in the spin case for larger periodicity.

TABLE III. Values for the spectral dimension D_s in the 3-periodic case for the plateau $l_{\min}^2 < \tau < l_{\max}^2$.

α	0.577	0.5765	0.576	0.5755
D_s	0.50 ± 0.01	1.40 ± 0.03	2.27 ± 0.02	3.17 ± 0.02

C. Analytical explanation of numerical results

The numerical result of a dimensional flow in cuboid spin foams can be explained in terms of the scaling of the amplitudes and an assumption on the scaling of the Laplacian.

The amplitude of cuboid spin foams scales in all cases with an exponent linear in the model's parameter α. In general, the vertex amplitude is a homogenous function of degree $-(a - b\alpha)$. The relevant instances here are $(a, b) = (9, 12)$ for spin variables $x_i = j_i$ according to Eq. (19) and $(a, b) = (14, 24)$ for the restriction to geometric configurations and a transformation to edge-length variables $x_i = l_i$, Eq. (21). Thus, expectation values in such a spin foam with V vertex amplitudes are sums over spin configurations weighted by

$$\mathcal{A} \propto \prod_v \hat{\mathcal{A}}_v^{(\alpha)}(\lambda\vec{x}) = \lambda^{-(a-b\alpha)V}\prod_v \hat{\mathcal{A}}_v^{(\alpha)}(\vec{x}). \tag{51}$$

In [17], a generic dimensional flow has been found for such superpositions weighted by a power-function measure $x^{-\gamma}$ in the case of a single variable x, summing from some

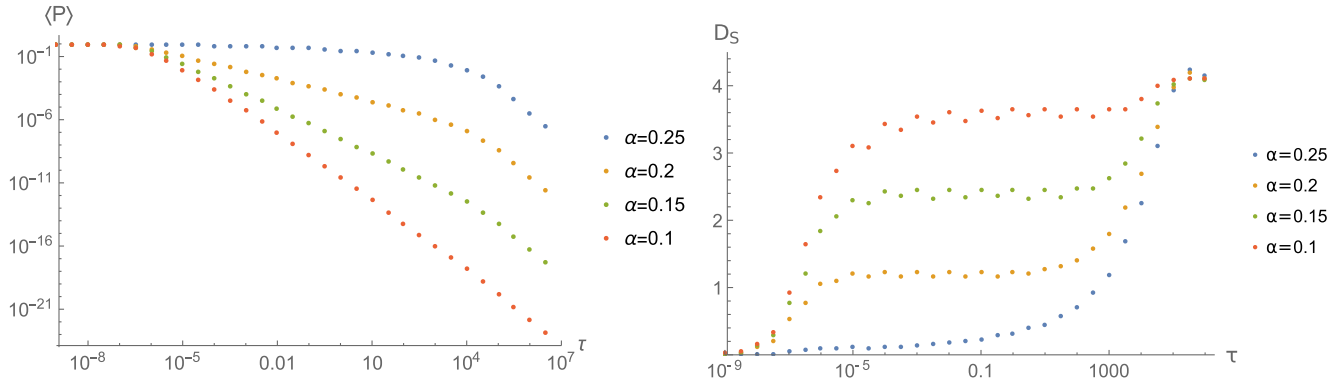

FIG. 5. Numerical results of $\langle P(\tau)\rangle$ (left) and D_s (right) in the 1-periodic case in spin variables for several values of α.

$x_{\min}$ to $x_{\max}$. If the Laplacian is a power function in this variable,

$$\Delta(x) = x^{-2\beta}\Delta, \tag{52}$$

where Δ is the purely combinatorial Laplacian on the hypercubic lattice, then one finds a dimensional flow from the topological dimension D at large scales, $\tau \gg x_{\max}^{2\beta}$, to a spectral dimension,

$$D_s = \begin{cases} 0, & \frac{\gamma-1}{\beta} \leq 0 \\ \frac{\gamma-1}{\beta}, & 0 < \frac{\gamma-1}{\beta} < D \\ D, & \frac{\gamma-1}{\beta} \geq D, \end{cases} \tag{53}$$

at small length scales $x_{\min}^{2\beta} \gg \tau \gg x_{\max}^{2\beta}$. For $\tau \ll x_{\min}^{2\beta}$ there is the usual falloff to 0 due to discreteness. Furthermore, the result of an intermediate dimension does not depend on the step size in the sum over x (as long as it is much smaller than $x_{\max}$). This result can be directly applied to the test case of a spin-foam sum restricted to equilateral ($n = 1$) configurations with $\gamma = (a - b\alpha)V$.

The equilateral result can now be generalized to the case of $\mathcal{N}$-periodic spin-foam configurations based on a scaling assumption for the Laplacian. For the spectrum of the Laplacian there is some evidence [49] that the scaling in a single variable Eq. (52) generalizes to $\mathcal{N}$-periodic lattices in terms of averages. That is, the assumption is that for a sufficiently large number n of independent length variables l_e on edges e [which depends in our setting on $\mathcal{N}$, see Eq. (67)],

TABLE IV. Values for the spectral dimension D_s in the 1-periodic case with spin variables for the plateau $l_{\min}^2 < \tau < l_{\max}^2$.

α	0.3	0.25	0.2	0.15	0.1
D_s	0.	0.121 ± 0.006	1.23 ± 0.02	2.42 ± 0.02	3.53 ± 0.02

$$\Delta(l_e) \approx \overline{l^2}^{-1}\Delta, \tag{54}$$

where $\overline{l^2}$ is the average over all squared edge lengths l_i^2 of a given configuration,

$$\overline{l^2} = \frac{1}{n}\sum_e l_e^2. \tag{55}$$

Under this assumption we can explain the numerical results analytically.

It should be emphasized that the scaling of the Laplacian's spectrum, though an assumption, is based on a well-motivated conjecture. In particular, this conjecture stems from an exact result on the perturbative expansion of the spectrum in the momentum k for any n [49]. For the spectral dimension, only the first (quadratic) order is relevant for obtaining the topological dimension above the discreteness scale. Subleading orders merely determine the form of a local maximum around the discreteness scale. Thus, the assumption is very meaningful in this context and the fact that the numerical results can be explained in this way further supports the conjecture.

The spin-foam expectation value of the heat trace can now be transformed to a one-dimensional integral, up to an irrelevant overall factor. We show this first for the restriction to geometric configurations where a transformation to edge-length variables l_e is possible and generalize then to arbitrary spins j_f. The key point is that a transformation of the integral

$$\langle P(\tau)\rangle = \frac{\int [\mathrm{d}l_e]^n \, \mathcal{A}(l_e)\mathrm{Tr}e^{\tau\Delta(l_e)}}{\int [\mathrm{d}l_e]^n \, \mathcal{A}(l_e)} \tag{56}$$

to "radial" coordinates with radius $\overline{l^2}$ is possible such that only the radial part contributes to the heat kernel expectation value. Explicitly, the transformation is

$$l_e = \sqrt{n\overline{l^2}} f_e(\Omega) \tag{57}$$

where $f_e(\Omega)$ are the standard angular functions in radial coordinates. In this way, the semiclassical cuboid spin-foam amplitudes factorize into a radial part and angular part $g(\Omega)$ as well,

$$\mathcal{A}(l_e) \propto \prod_v \hat{\mathcal{A}}_v^{(\alpha)}(l_e) = \sqrt{n\overline{l^2}}^{-(a-b\alpha)V} g(\Omega). \quad (58)$$

Then, the angular part in the heat-trace expectation factorizes and cancels with the denominator

$$\langle P(\tau)\rangle_\alpha = \frac{\int_{l_{\min}}^{l_{\max}} [\mathrm{d}l_e]^n \prod_v \hat{\mathcal{A}}_v^{(\alpha)}(l_e) \mathrm{Tr} e^{\tau\Delta(l_e)}}{\int_{l_{\min}}^{l_{\max}} [\mathrm{d}l_e]^n \prod_v \hat{\mathcal{A}}_v^{(\alpha)}(l_e)}$$
$$\approx \frac{\int_{l^2_{\min}}^{l^2_{\max}} \mathrm{d}\overline{l^2}\, \sqrt{\overline{l^2}}^{n-2-(a-b\alpha)V} \mathrm{Tr} e^{\tau\overline{l^2}^{-1}\Delta}}{\int_{l^2_{\min}}^{l^2_{\max}} \mathrm{d}\overline{l^2}\, \sqrt{\overline{l^2}}^{n-2-(a-b\alpha)V}} \quad (59)$$

$$= \frac{1}{{l_{\max}}^{n-(a-b\alpha)V} - {l_{\min}}^{n-(a-b\alpha)V}} \times \int_{l^2_{\min}}^{l^2_{\max}} \mathrm{d}\overline{l^2}\, \sqrt{\overline{l^2}}^{n-2-(a-b\alpha)V} \mathrm{Tr} e^{\tau\overline{l^2}^{-1}\Delta}. \quad (60)$$

For the remaining part one can apply again the result Eq. (53) from [17], now with $\beta = 1/2$ and $\gamma = (2 + (a - b\alpha)V - n)/2$ such that there is a dimensional flow to

$$D_s^\alpha = V(a - b\alpha) - n \quad (61)$$

at $l^2_{\min} \ll \tau \ll l^2_{\max}$ for $0 < V(a - b\alpha) - n < D$. Note that in this way any value $D_s^\alpha \in [0, D]$ can be obtained for some α for a finite number of degrees of freedom n and vertex amplitudes V. The range of α where such a flow occurs is given by

$$\alpha = \frac{1}{b}\left(a - \frac{n}{V}\right) - \frac{1}{bV} D_s^\alpha. \quad (62)$$

Numerical calculations in the various cases are in perfect agreement with the analytically derived linear relationship between D_s^α and the theory's parameter α, as shown in Fig. 6.

It is not obvious, however, how the scaling of the Laplacian generalizes from the case of length variables to area variables, Eq. (37), and thus spins j_f. At first, a scaling in $\overline{j_f}$ or in $\overline{j_f^2}$ seems meaningful. Here we take our numerical results as input where we find a dimensional flow for the sum over n spins j_f (see Fig. 6) to

$$D_s^\alpha = 2(V(a - b\alpha) - n). \quad (63)$$

This can be explained under the assumption for the Laplacian on spin configurations

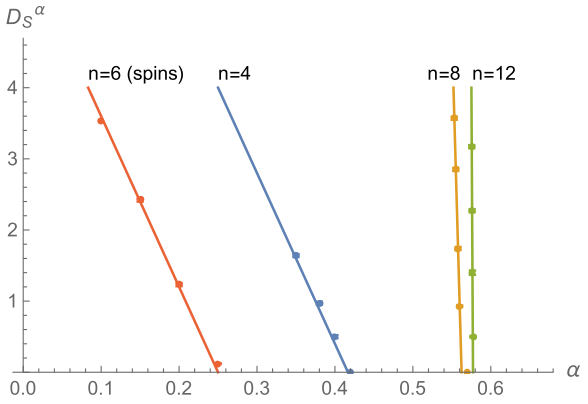

FIG. 6. Comparison of numerical results (values and error bars according to Tables I–IV) with the analytical result Eqs. (61) and (63) for the intermediate spectral dimension D_s^α as a function of the model parameter α for $n = 4$ ($V = 1$), $n = 8$ ($V = 16$) and $n = 12$ ($V = 81$) length variables, as well as $n = 6$ ($V = 1$) spin variables.

$$\Delta(j_f) = \overline{j^2}^{-1/2}\Delta \quad (64)$$

which means that $\overline{j^2} = \frac{1}{n}\sum j_f^2$ is the proper average for the scaling assumption. Performing the same transformation to radial-type coordinates, now in the space of spin configurations,

$$\mathcal{A}(j_f) \propto \prod_v \hat{\mathcal{A}}_v^{(\alpha)}(j_f) = (n\overline{j^2})^{-(a-b\alpha)V/2} h(\Omega), \quad (65)$$

one finds the heat-trace expectation value

$$\langle P(\tau)\rangle \propto \int_{j_{\min}}^{j_{\max}} [\mathrm{d}j_f]^n \prod_v \hat{\mathcal{A}}_v^{(\alpha)}(j_f) \mathrm{Tr} e^{\tau\Delta(j_f)} \approx \frac{1}{2}\sqrt{n}^n \times \int \mathrm{d}\Omega \prod_v h_v(\Omega) \int_{j^2_{\min}}^{j^2_{\max}} \mathrm{d}\overline{j^2}\, (\overline{j^2})^{\frac{n-2-(a-b\alpha)V}{2}} \mathrm{Tr} e^{\tau\overline{j^2}^{-1/2}\Delta}. \quad (66)$$

Thus, the only difference in the resulting equation for the intermediate dimension D_s^α between a spin-foam sum over spins j_f and the restricted spin-foam sum over geometric configurations given by l_e is a factor of 2 stemming from the different scaling of Laplacian in the squared-variable average, that is $\beta = 1/4$ for spins and $\beta = 1/2$ for edge lengths.

Accordingly, there is an effect of nongeometricity in this spin-foam model on the spectral dimension, though the underlying reason seems to be the number of degrees of freedom and resulting amplitude scaling rather than an explicitly geometric explanation. The number of degrees of freedom on the $\mathcal{N}$-periodic configurations of the cuboid spin-foam model with its translation invariance is $n = \binom{D}{2}\mathcal{N}^2$ for spin variables on faces, or $n = D\mathcal{N}$ for length

variables on edges. Together with the different amplitude scaling (a, b), Eq. (51), one finds a different $\mathcal{N}$-dependent offset in the linear relation between D_s^α and α, while the slope is the same in both cases for given $\mathcal{N}$ (see Fig. 6). Restricting to geometric configurations shifts the range of α at which a dimensional flow occurs to smaller α for $\mathcal{N} \geq 2$. This is true in particular for the large-$\mathcal{N}$ limit which we discuss in the following.

IV. FULL CUBOID-SPIN-FOAM SUM AND RENORMALIZATION GROUP FLOW

Though the analytic equations explaining our numerical results turn out to be rather simple, the physical consequences are far reaching. In the end we are interested in the large-periodicity limit, that is, the full cuboid spin-foam sum. The analytic equations Eqs. (61) and (63) allow us to take this limit. It appears that the range of α where an intermediate dimension $0 < D_s^\alpha < D$ is observed shrinks to a point $\{\alpha_*\}$. We provide two interpretations for this fact. Considering the large-periodicity limit as a certain thermodynamic limit, one can argue that $\alpha = \alpha_*$ is the point in the parameter space of such a model where a phase transition from zero-dimensional to D-dimensional spacetime takes place. Complementary, one can ask the question whether our results are consistent across lattices of different periodicity. In this sense we discuss the possibility to use D_s^α as a condition to define a renormalization group flow for α. We discuss these two possibilities—which should be emphasized not to be exclusive subsequently—in the two parts of this section. In any case, an intriguing aspect is that dynamics, more precisely the amplitude $\hat{\mathcal{A}}_v^{(\alpha)}$, at α_* is invariant under global rescaling, connecting the discussion also with the topic of restoration of diffeomorphism invariance.

A. The large-$\mathcal{N}$ limit and scale invariance

Our numerical computations are approximate in a twofold way. For explicit calculations one has to fix a finite $\mathcal{N}$ and a finite maximal spin $j_{\max}$. To obtain exact results it is necessary to take the limits $\mathcal{N} \to \infty$ and $j_{\max} \to \infty$. The main advantage of the analytic explanation of the results under the power-law assumption for the Laplacian is that they enable us to take these limits.

Both our numerical and analytical studies reveal a universal behavior of the spectral dimension for cuboid spin foams. For any choice of finite number of spin-foam vertices V or finite periodicity $\mathcal{N}$ we observed essentially three different regimes depending on the parameter α: For large α we observe $D_s = 0$, for small $\alpha D_s = D$ and in between those regions exists a small interval in which D_s can take any value between 0 and D changing continuously with α. However, the position and size of this interval in α depend sensitively on the size of spin foam. For growing $\mathcal{N}$ (or V) the size of this interval shrinks and the upper and lower end increase to approach the value in α where the spin-foam amplitude becomes invariant under global scaling, i.e. $\hat{\mathcal{A}}(\{\lambda j_i\}) = \hat{\mathcal{A}}(\{j_i\})$.

Thus, the relevant quantity to analyze is the parameter $\alpha = \alpha_{\mathcal{N}}(D_s^\alpha)$ at which a certain intermediate dimension D_s^α is observed for $\mathcal{N}$-periodic spin-foam configurations. When approximating large spin-foam configuration sums by $\mathcal{N}$-periodic configurations, the details of the limit depend on the specific degrees of freedom. On a hypercubic spin-foam lattice there are in general $n \propto \mathcal{N}^D$ degrees of freedom. However, because of the translation invariance Eq. (30) due to the restriction to cuboids this reduces to

$$n = c_D \mathcal{N}^p \tag{67}$$

where $p = 2$ and $c_D = \binom{D}{2}$ for a general spin configuration while $p = 1$ and $c_D = D$ for edge-length variables in the restriction to geometric configurations. In any case it is meaningful to restrict the dynamics according to the periodicity, that is $V = \mathcal{N}^D$ vertex amplitudes. As a result, the generalized version of Eq. (62) is

$$\alpha_{\mathcal{N}}(D_s^\alpha) = \frac{a}{b} - \frac{c_D}{b}\mathcal{N}^{-D+p} - \frac{2\beta}{b} D_s^\alpha \mathcal{N}^{-D} \tag{68}$$

where $\beta = 1/4$ in the general spin case and $\beta = 1/2$ in the geometric edge-length case, as discussed before. While any value $D_s^\alpha \in [0, D]$ can be obtained for some α for a finite number of degrees of freedom, there is a fine-tuning with the periodicity $\mathcal{N}$. The larger the $\mathcal{N}$, the smaller the range of α yielding an intermediate dimension D_s^α. In particular, in the limit $\mathcal{N} \to \infty$, this α-interval shrinks to a point $\alpha_* = a/b$.

The discontinuous jump from $D_s^\alpha = 0$ to $D_s^\alpha = D$ at α_* in the limit $\mathcal{N} \to \infty$ is reminiscent of a phase transition. First of all, one can indeed consider the large-$\mathcal{N}$ limit as a thermodynamic limit. It is the limit of a large number of degrees of freedom according to Eq. (67). While in quantum gravity volume becomes a quantum observable itself; its expectation value, being an extensive quantity, is expected to scale with the combinatorial size N_{lattice} of the lattice underlying the spin-foam configurations, in particular, with the number of vertices such that their ratio is fixed. For technical reasons, i.e. to avoid the compactness effect of the spectral dimension, we have considered $\mathcal{N} \ll N_{\text{lattice}}$ in explicit, finite-$\mathcal{N}$ computations in Sec. III. In the large-$\mathcal{N}$ limit it is however equally meaningful to consider lattices of size $N_{\text{lattice}} = \mathcal{N}$. In this sense, $\mathcal{N} \to \infty$ is indeed a thermodynamic limit.

Certainly, the quantity of spacetime dimension is a suitable order parameter in the broadest sense to describe the properties of different phases of a quantum geometry. A different (effective) dimension of a spacetime, in particular, when this spacetime is made up of intrinsically D-dimensional building blocks, implies that it is ordered in

a different way. The spectral dimension D_s captures a particularly physical aspect of spacetime dimension, i.e. the effective dimension as tested by a scalar field. Hence the spectral dimension is a highly nonlocal quantity encapsulating information of the entire spacetime. However this is not surprising in theories of quantum gravity which are expected to have nonlocal features, e.g. due to diffeomorphism invariance. Thus the definition of physically meaningful local quantities is rather challenging. In causal dynamical triangulations, for comparison, it is also common to use averaged geometric quantities such as the number of triangulation vertices per number of 4-cells as order parameters [18]. These quantities have a more precise meaning as order parameters since they are conjugate to coupling parameters on the level of the state sum. Still, the jump of the spectral dimension from $D_s^\alpha = 0$ to $D_s^\alpha = D$ at $\alpha = \alpha_*$ is at least a strong sign for a phase transition.

The phase transition to D-dimensional spacetime becomes even more relevant in the large-$j_{\max}$ limit. The scale of the dimensional flow from D to $D_s^\alpha \leq D$ is given by the largest length scale $l_{\max}^2 \sim j_{\max}$ up to which the spin foam is summed. However, this is just an artificial cutoff, to be sent to infinity in most spin-foam models.[9] As a consequence, this flow from D_s^α to D is shifted to infinity, that is, the spectral dimension has the value D_s^α on all scales (above the discreteness scale $j_{\min}$). In particular, for an α yielding $D_s^\alpha < D$ semiclassical quantum spacetime is indeed of dimension smaller than the observed classical D-dimensional spacetime. The usual D dimensions occur only below some minimal $\alpha_{\min}$, either continuously for finite $\mathcal{N}$, or discontinuously at $\alpha = \alpha_*$ in the thermodynamic limit $\mathcal{N} \to \infty$. In this sense D-dimensional spacetime emerges in this spin-foam model.

The critical parameter α_* has a special physical relevance, as it is the point where the amplitude $\hat{\mathcal{A}}_v^{(\alpha)}$ becomes invariant under global rescaling; i.e. only the shape of the cuboid determines the value of the amplitude, not its scale. Indeed we know from [43,45] that α determines whether small or large spins are preferred in the spin-foam state sum, where α_* marks the turning point between these two domains.

This tells us that in the $\mathcal{N} \to \infty$ limit, the spectral dimension D_s is solely determined by the global scaling behavior of the amplitude, where the scale-invariant amplitude marks the transition between the phases characterized by $D_s = 0$ and $D_s = 4$. The individual shape of the cuboids does not seem to influence the spectral dimension. Interestingly, this observation strongly resonates with the action of an Abelian subgroup of diffeomorphisms, which transforms a cuboid configuration into another cuboid configuration. Such a diffeomorphism acts by shifting an entire hyperplane in the direction orthogonal to it to obtain another hypercubioid configuration. Hence such a diffeomorphism only changes how flat space is subdivided into flat cuboids, which are glued together in a flat way.

The independence of the spectral dimension on the shape of the cuboids in the $\mathcal{N} \to \infty$ limit implies that it is indeed invariant under such diffeomorphisms which might indicate that diffeomorphism invariance is restored in this limit at $\alpha = \alpha_*$. This is further underlined by two previous results on cuboid spin foams restricted to geometric configurations. In [43] two glued hypercuboids were considered under translations of the middle cube along which they are glued while keeping the total volume fixed. It was found that $\hat{\mathcal{A}}_v^{(\alpha)}$ is almost invariant under such hyperplane translations for $\alpha \approx 0.6$. Similarly in [44,45] indications for a UV-attractive fixed point of the renormalization group flow of $\hat{\mathcal{A}}_v^{(\alpha)}$ were found around $\alpha \approx 0.628$. It has been conjectured that broken diffeomorphism symmetry of discrete theory gets restored at such a fixed point [79,80]. Remarkably both these values are in close proximity to $\alpha_* = 14/24 \approx 0.583$ in the present context. The root of the discrepancy might be due to the fact that the calculations in [43,45] were performed for finite lattices, whereas our result holds for $V, \mathcal{N} \to \infty$.

Conversely, we can revert the logic and wonder when to expect a nontrivial spectral dimension. In our study of the spectral dimension for finite periodicity $\mathcal{N}$ of the spin foam, we observed two different regimes in α, one with $D_s = 0$ and one with $D_s = 4$ separated by a small region in which it changes continuously. In the limit of $\mathcal{N} \to \infty$ the two regimes persist and we can readily assign a spectral dimension to them. However the intermediate region, which contains any $0 < D_s < 4$, shrinks to a single point α_*. Hence we cannot infer a value of the spectral dimension right on this transition, yet we expect it to be nontrivial there. Moreover, if this is the point on which diffeomorphism symmetry is restored, we conjecture that the spectral dimension shows a nontrivial behavior there.

Naturally, this reasoning should be taken with a grain of salt. The spectral dimension is, by definition, a global and nonlocal observable, in which many properties of a geometry get washed out. This is even more true in the case of a quantum geometry where one sums over all geometries allowed by the theories. Nevertheless, the fact that in the $\mathcal{N} \to \infty$ limit only the scaling properties of the amplitude determine the spectral dimension and microscopic properties do not appear to play any role hints towards a restoration and connection to diffeomorphism invariance.

As an exception, spin-foam configurations on a hypercubic lattice without any symmetry on the variables are a special case with a slightly different limit α_*. While the cuboid spin-foam model implies translation invariance, our analytical argument also applies to less restricted spin-foam sums. If all variables in the spin-foam configurations are independent, that is $p = D$ in Eq. (67), the $\alpha_{\mathcal{N}}(D_s^\alpha)$ relation Eq. (68) is modified and has the limit

[9] Spin-foam models for quantum gravity with a nonvanishing cosmological constant Λ often come with a natural cutoff $j_{\max}$ on the spins [71–78]. One possibility is quantum groups at the root of unity, where $j_{\max}$ is related to the level k of the quantum group.

$$\alpha_{\mathcal{N}}(D_s^\alpha) = \frac{a - c_D}{b} - \frac{2\beta}{b} D_s^\alpha \mathcal{N}^{-D} \underset{\mathcal{N}\to\infty}{\to} \frac{a - c_D}{b} \quad (69)$$

corresponding to a shift $a \mapsto a - c_D$. No such spin-foam model with $n \propto \mathcal{N}^D$ variables has been calculated explicitly yet. But it is obvious that such a model, being much less restricted than the cuboids, would describe also curvature and other degrees of freedom. One could take this simple argument for a different α_*, thus as a hint that such a model would indeed also be scale invariant at such nontrivial α_*.

B. Renormalization and the spectral dimension as order parameter

Complementary to the thermodynamic limit $\mathcal{N} \to \infty$ one can pose the question of how the results depend on the chosen periodicity $\mathcal{N}$ and whether the results for the spectral dimension are consistent. Indeed, spin foams of different periodicity correspond to different choices of discretizations. Generically, for the same α, we then obtain different values for the spectral dimension for different periodicities $\mathcal{N}$. To make this consistent, we can revert the reasoning and ask which α, i.e. which spin-foam amplitudes, must we assign to spin foams of different periodicity in order to observe the same spectral dimension. In this sense, we use the value of the spectral dimension as a criterion to define a renormalization group flow for different periodicities, namely for finer and coarser discretizations. If we then consider the flow in the refining direction, i.e. growing $\mathcal{N}$, we reobtain the large-$\mathcal{N}$ limit and observe the flow $\alpha \to \alpha_*$ for all $0 < D_s < 4$. In this sense we can interpret α_* as the UV fixed point of the renormalization group flow.

In a nutshell, the idea behind renormalization in spin foams is to model the same physical transition on different discretizations. This is done by relating and identifying boundary states across Hilbert spaces by embedding maps and looking for consistent dynamics [39–42,48]. This naturally extends to expectation values of observables, which should be the same for different discretizations. Conversely one can invert this logic and define a renormalization group flow by requiring that expectation values of observables agree [43–45]. The spectral dimension, which is a global observable defined for all discretizations, is a possible candidate (with certain limitations[10]).

In this article we have studied infinite four-dimensional lattices without a boundary; hence the refining formalism via embedding maps does not readily apply. As a further restriction we have set the spin foam to be $\mathcal{N}$ periodic to have better control over the number of variables. A natural idea to relate the spectral dimension across such discretizations is to compare an $\mathcal{N}$-periodic spin foam to a $2\mathcal{N}$-periodic one.

This comparison works conceptually as follows: The $2\mathcal{N}$-periodic spin foam is regarded as the refinement of the $\mathcal{N}$-periodic one. This implies that each of the repeated cells is subdivided once in each dimension, resulting in 2^D times more lattice sites for the $2\mathcal{N}$-periodic spin foam. For this comparison to be reasonable, we must ensure that we compare the spectral dimension for similar (superpositions of) geometries.

For the cuboid spin foams studied here, the only relevant geometric quantity is the spins on faces, or the lengths on edges in the geometric restriction. Thus our results so far are labeled by the minimal and maximal allowed spins $j_{\min}$, $j_{\max}$ or edge lengths $l_{\min}$, $l_{\max}$. In order to compare $\mathcal{N}$- and $2\mathcal{N}$-periodic lattices, their total minimal and maximal scales must agree. For geometric cuboids this naturally implies that the minimal and maximal lengths in the $2\mathcal{N}$-periodic case are just half the size of their respective counterparts in the $\mathcal{N}$-periodic case. Accordingly, for spins which relate to areas the refinement step yields

$$j_{\min} \mapsto \frac{1}{\sqrt{2}} j_{\min}, \qquad j_{\max} \mapsto \frac{1}{\sqrt{2}} j_{\max}. \quad (70)$$

In this sense the $2\mathcal{N}$-periodic configuration is a refinement of the $\mathcal{N}$-periodic one via a rescaling.

The comparison of the spectral dimension across spin foams of different periodicity $\mathcal{N}$ leads to a flow in α as follows: From the analytical explanation of our numerical results we have an explicit formula for the intermediate spectral dimension $D_s^\alpha = D_s^\alpha(\alpha, \mathcal{N})$ as a function of α and $\mathcal{N}$, via the number of vertices $V = \mathcal{N}^D$ and number of degrees of freedom $n = c_D \mathcal{N}^p$ with $0 < p \leq D$ covering all the possible cases discussed in Sec. IV A. If D_s is supposed to be the same under refining $\mathcal{N}_{i+1} = 2\mathcal{N}_i$, we have to assign specific parameters $\alpha_i = \alpha_{\mathcal{N}_i}$ and $\alpha_{i+1} = \alpha_{\mathcal{N}_{i+1}} = \alpha_{2\mathcal{N}_i}$ to each periodicity. Then we interpret the $\mathcal{N}_i$-periodic spin foam for α_i as the effective, coarse-grained amplitude of the $\mathcal{N}_{i+1}$-periodic spin foam for α_{i+1}, both giving rise to the same spectral dimension D_s^α. According to Eqs. (61) and (63) the parameters α_i have to satisfy

$$\begin{aligned} 2\beta D_s^\alpha(\alpha_i, \mathcal{N}_i) = (a - b\alpha_i)\mathcal{N}_i^D - c_D \mathcal{N}_i^p = 2\beta D_s^\alpha(\alpha_{i+1}, \mathcal{N}_{i+1}) &= (a - b\alpha_{i+1})\mathcal{N}_{i+1}^D - c_D \mathcal{N}_{i+1}^p \\ &= (a - b\alpha_{i+1}) 2^D \mathcal{N}_i^D - c_D 2^p \mathcal{N}_i^p \end{aligned} \quad (71)$$

[10]For the spectral dimension to show meaningful behavior, one cannot choose the underyling discretization to be too small. Otherwise one only observes the compactness of geometry; see also the discussion in Sec. II C.

or equivalently

$$(a - b\alpha_{i+1}) - 2^{-D}(a - b\alpha_i) = c_D 2^{-D}(2^p - 1)\mathcal{N}_i^{p-D}. \tag{72}$$

For $p < D$ the right-hand side vanishes for large $\mathcal{N}$. The equation is then solved by

$$\alpha_i = \frac{a}{b} - \frac{1}{2^{D(i-1)}}\left(\frac{a}{b} - \alpha_0\right) \underset{i\to\infty}{\to} \frac{a}{b} \tag{73}$$

which converges to $\alpha_* = a/b$ after many refinement steps, independent of some initial parameter value $\alpha = \alpha_0$. Taking the $\mathcal{N}$-dependent right-hand side of Eq. (72) into account, the more general flow depending on $\mathcal{N}_i = 2^i\mathcal{N}_0$ is

$$\alpha_i = \frac{a}{b} - \frac{1}{2^{D(i-1)}}\left(\frac{a}{b} - \alpha_0\right) - \frac{1}{\mathcal{N}_i^{D-p}}\left(1 - \frac{1}{2^{D(i-1)}}\right)\frac{2^p - 1}{2^D - 1}\frac{c_D}{b}. \tag{74}$$

In particular, one observes that for a full set of independent variables, $p = D$, and only in this case, the fixed point of the flow is shifted to $\alpha_* = (a - c_D)/b$, in agreement with Eq. (69).

Remarkably, this result does not depend on the scaling of the Laplacian captured by β. Furthermore, the details of the coarse graining are not important either. Any refinement $\mathcal{N}_{i+1} = \kappa\mathcal{N}_i$, $\kappa > 1$, leads to the same fix point α_* (where formally κ might even be real). The kinds of variables of the models captured by p and c_D, in particular, length or spin variables, make a difference only if $p = D$, that is, if the number of variables are proportional to the number of vertex amplitudes.

There is subtlety regarding the consistency of the flow equations Eq. (72). For a given value of intermediate dimension $0 < D_s^\alpha < D$, there exists only one value α for any (finite) periodicity producing this spectral dimension. Thus, the renormalization group flow $\alpha_i \to \alpha_{i+1}$ is unambiguous and actually invertible. However, for $D_s^\alpha = 0$ or $D_s^\alpha = 4$ we usually find large domains in α giving such a spectral dimension. Consequently when considering the flow, no unambiguous flow can be defined directly. This quite significantly restricts the applicability of Eq. (72) as the α interval permitting $0 < D_s^\alpha < D$ shrinks rapidly.

Nevertheless, one can extend the flow to all α covering also the regime of $D_s = 0$ and $D_s = 4$. On these values it is never going to flow out of this phase by the renormalization group flow. Hence we can define a new α_i under renormalization for it by considering the minimal value $\alpha_i(D_s^\alpha = 0)$ for $D_s^\alpha = 0$ as well as the maximal value $\alpha_i(D_s^\alpha = 4)$. If we have $D_s^\alpha = 0$, the α_i to be renormalized is $\alpha_i \geq \alpha_i(0)$, whereas for $D_s = 4$, the corresponding $\alpha_i \leq \alpha_i(4)$. In this sense, we can extend Eq. (72) to the entire domain of α.

At this stage, a comment on the flow itself is in order. Given the previously mentioned extension, we always see a flow under refinement of $\alpha \to \alpha_*$. In that sense the flow is UV attractive. However, this statement should be taken with a grain of salt. It clearly holds that if we start, for a given $\mathcal{N}$, with an α leading to a $0 < D_s < 4$, yet outside this interval, which quickly shrinks for growing $\mathcal{N}$, we have defined the flow to be the same as inside the interval. This behavior might indicate that the spectral dimension is not an ideal observable to define a renormalization group flow, but still serves as a good order parameter for identifying different geometric phases of the model.

Note that this renormalization group flow is defined under the assumption that the Laplace operator—and thus the way the scalar field probes spacetime—does not change under this flow, which is well motivated by regarding the scalar field as a mere test field. However, in general *both* matter and gravity need to be renormalized at the same time, e.g. to describe how matter effectively propagates on an effective spacetime. Furthermore it is necessary to identify consequences of choosing a particular discrete Laplace operator. We hope to shed more light on these intriguing questions in future research.

V. CONCLUSIONS

In this work we have calculated the spectral dimension of flat quantum spacetime as defined by the restriction of the EPRL-FK spin-foam model to cuboid geometries. More precisely we studied $\mathcal{N}$-periodic spin foams, both numerically and analytically, and found the following general behavior: The spectral dimension vanishes below the minimal scale $j_{\min}$ and flows to $D_s = 4$ above a maximal scale $j_{\max}$. In between we have found an intermediate value $0 \leq D_s^\alpha \leq 4$ that depends sensitively on the parameter α characterizing the face amplitude of the spin-foam model as well as the number of degrees of freedom n parametrized by the periodicity $\mathcal{N}$. For larger α, we always find $D_s^\alpha = 0$, whereas $D_s^\alpha = 4$ for small α. In between, for finite $\mathcal{N}$, there exists an interval in α in which D_s^α increases linearly with decreasing α. This interval shrinks with increasing $\mathcal{N}$. Under the assumption that the Laplacian scales with a certain power of the inverse mean square of the spin-foam variables we have analytically derived the relation between D_s^α and α for arbitrary periodicity $\mathcal{N}$ which is in good

agreement with our numerical results. This allows us to generalize our numerical results to any $\mathcal{N}$. It furthermore predicts the results for models on a lattice with different variables, e.g. fewer symmetries.

The analytical results permit us to take the $\mathcal{N} \to \infty$ limit in which the α-interval of intermediate dimensions D_s^α shrinks to a point marking a discontinuous transition between $D_s = 0$ and $D_s = 4$. We have interpreted this as evidence for a phase transition from zero-dimensional to four-dimensional spacetime. The point of this transition is precisely given by $\alpha = \alpha_*$ on which the spin-foam amplitudes become invariant under global rescaling. Hence the spectral dimension in the $\mathcal{N} \to \infty$ limit solely depends on the scaling behavior of the amplitude and not on the shape of the individual cuboids. This hints towards restoration of (an Abelian subgroup of) diffeomorphisms in this limit. To the best of our knowledge, this is the first time that such an emergence of four-dimensional spacetime has been found in the context of spin-foam models.

Naturally these results must be taken with a grain of salt: the cuboid spin-foam model we considered here is a restricted version of the EPRL-FK model. We define it on a hypercubic lattice and fix the intertwiners to be of cuboid shape. Thus, in the large-j limit these lattices are essentially flat geometries, which are subdivided in different ways. As a consequence, several features which we expect to influence the spectral dimension are not accessible in this model. Intertwiner degrees of freedom, encoding different shapes of three-dimensional building blocks, are not summed over, and thus we cannot encode curvature. As another consequence, the model is not sensitive to oscillating spin-foam amplitudes. Furthermore, we have not studied the deep quantum regime by restricting ourselves to the large-j limit, such that log oscillations as proposed to be a general feature of quantum geometry [81] are not observed. Anyway, on sufficiently large length scales the spectral dimension is not affected by quantum (small-spin) effects since short scale geometries get exponentially suppressed in the return probability for growing diffusion time. In spite of these restrictions, we expect our results to carry over qualitatively to more general spin-foam models (for Riemannian signature on semiclassical length scales).

However, the spectral dimension is very sensitive to the combinatorial structure of a discrete or discretized spacetime theory. Beyond regular lattices as exploited here, it remains a huge challenge to find at all ensembles of combinatorially random geometries which are effectively four dimensional [82,83]. So far, only severe constraints on the combinatorics of the cell complexes such as a foliation into spatial hypersurfaces as in causal dynamical triangulations [9,18], or combinatorial translation invariance as in the hypercubic lattice, are known to lead to a regime of $D_s = 4$. The use of such a lattice is very meaningful in the present context where spin-foam configurations are considered as a discretization of continuum spacetime and the dynamics are eventually defined through coarse graining and a renormalization group flow. On the other hand, our results have no straightforward generalization to a context where different combinatorial ensembles dominate, for example triangulations dual to melonic diagrams as in tensor models [84–86]. Since such triangulations effectively obey the structure of branched polymers [87], one would expect also for a spin-foam model with such combinatorics a maximal value of the spectral dimension of $D_s = 4/3$. In this sense, the expectation that our results still hold on more general spin-foam models applies to a generalization of the variables on a lattice, not to a generalization of the lattice to any other combinatorial dynamics.

Despite these limitations, our model allows us to isolate one particular aspect of spin foams affecting the spectral dimension, namely the superposition of geometries. Indeed, most of the single discrete geometries summed over in the path integral have a spectral dimension $D_S = 4$ above their respective effective lattice scale given by the spins. Hence, one might not be surprised to find a phase with $D_S = 4$ for the quantum geometry. However, we have observed that depending on the spin-foam amplitude the quantum geometry is described by $D_S < 4$ or that it might even be zero dimensional. The latter occurs when the amplitude prefers large spins while an intermediate value is the effect of a subtle balance of spins of all sizes. If a regime with $D_S = 4$ is supposed to appear in general in spin-foam models, it occurs where this balance tends towards a preference of small spins in the partition function.

Furthermore, in the more general spin case our model allows for nongeometric configurations, which can be interpreted as torsion. However, despite quantitative differences we have not observed a qualitatively different behavior from the geometric case. In this way we would also like to see our work as a proof of principle upon which to build future research on. One crucial idea for our work is to use periodic configurations. From the numerical perspective it is the indispensable ingredient to build feasible simulations by keeping the number of variables reasonably small. Moreover it allowed us to study the full spectrum of the Laplacian and avoid the issue of compactness of the configurations. We are curious to see whether these ideas are applicable to more scenarios in spin-foam models.

We expect these results to transfer qualitatively also to more general spin-foam models, at least for Riemannian signature. The cuboid restriction of the EPRL model is a restriction to flat spacetime on the level of the quantum state sum. An obvious next step in this line of research would be to compute the spectral dimension on less restricted models which cover curvature degrees of freedom, for example the frustrum model [47] with cosmological constant [88]. Still, our guess would be that local curvature excitations do not effect the qualitative behavior of the spectral dimension as a global observable. Already in

the cuboid model computed here there are torsionlike degrees of freedom due to the nongeometricity. We have seen that their main effect as compared to the restriction to geometric configurations is only a quantitative modification to the α-dependence of the result, which is eventually due to the different number of degrees of freedom. We expect similar modifications when adding more local degrees of freedom such as curvature.

Extending our study to models for Lorentzian signature is more challenging for several reasons. One is simply that the large-spin asymptotics for the Lorentzian model is known only partially and the case of cuboid restriction remains to be worked out. Another reason is that, if one considers the field propagation as actually physical, the possibility to return to the same point in spacetime in the Lorentzian context would imply closed-timelike curves or random walkers propagating back in time. This issue could be addressed transferring the definition of causal spectral dimension as studied in causal sets [21] to spin foams. On the contrary, one could argue that a notion of dimension should not directly depend on the causal structure. In fact, the definition of the quantum spectral dimension depends only on the spectral properties of the geometry (implicit in the Laplacian) and the quantum dynamics as captured by the spin-foam amplitude. The causal structure is then already induced by the spectrum of Lorentzian Laplacians and Lorentzian amplitudes.

ACKNOWLEDGMENTS

S. S. thanks Lisa Glaser for encouraging him to study the spectral dimension in spin foams. J. T. thanks Benjamin Bahr and the II Institute for Theoretical Physics at the University of Hamburg for hospitality at the initial stage of this work. The authors thank Benjamin Bahr, Lisa Glaser, Bianca Dittrich, Sylvain Carrozza, Lee Smolin, Renate Loll, Jan Ambjørn, Timothy Budd, Astrid Eichhorn, Sumati Surya, Frank Saueressig and Hanno Sahlmann for enlightening discussion during various stages of this work. S. S. was supported in part by the Perimeter Institute for Theoretical Physics. Research at the Perimeter Institute is supported by the Government of Canada through Innovation, Science and Economic Development Canada and by the Province of Ontario through the Ministry of Research, Innovation and Science. S. S. was further supported by Grant No. BA 4966/1-1 of the German Research Foundation (DFG). J. T. was supported by the German Academic Exchange Service (DAAD) with funds from the German Federal Ministry of Education and Research (BMBF) and the People Programme (Marie Curie Actions) of the European Union's Seventh Framework Programme (Grant No. FP7/2007-2013) under REA Grant No. 605728 [Postdoctoral Researchers International Mobility Experience (P.R.I.M.E.)].

[1] D. Oriti, Disappearance and emergence of space and time in quantum gravity, Studies in History and Philosophy of Modern Physics, **46**, 186 (2014).
[2] K. Crowther, Appearing out of nowhere: The emergence of spacetime in quantum gravity, Ph.D. thesis, University of Sydney, 2014.
[3] F. Caravelli, A. Hamma, F. Markopoulou, and A. Riera, Trapped surfaces and emergent curved space in the Bose-Hubbard model, Phys. Rev. D **85**, 044046 (2012).
[4] S. Rastgoo and M. Requardt, Emergent spacetime via a geometric renormalization method, Phys. Rev. D **94**, 124019 (2016).
[5] S. J. Carlip, Dimension and dimensional reduction in quantum gravity, Classical Quantum Gravity **34**, 193001 (2017).
[6] L. Crane and L. Smolin, Spacetime foam as the universal regulator, Gen. Relativ. Gravit. **17**, 1209 (1985).
[7] L. Crane and L. Smolin, Renormalization of general relativity on a background of spacetime foam, Nucl. Phys. **267**, 714 (1986).
[8] J. Ambjorn, J. Jurkiewicz, and R. Loll, The Spectral Dimension of the Universe is Scale Dependent, Phys. Rev. Lett. **95**, 171301 (2005).
[9] J. Ambjorn, J. Jurkiewicz, and R. Loll, Reconstructing the Universe, Phys. Rev. D **72**, 064014 (2005).
[10] D. N. Coumbe and J. Jurkiewicz, Evidence for asymptotic safety from dimensional reduction in causal dynamical triangulations, J. High Energy Phys. 03 (2015) 151.
[11] O. Lauscher and M. Reuter, Fractal spacetime structure in asymptotically safe gravity, J. High Energy Phys. 10 (2005) 050.
[12] P. Horava, Spectral Dimension of the Universe in Quantum Gravity at a Lifshitz Point, Phys. Rev. Lett. **102**, 161301 (2009).
[13] D. Benedetti, Fractal Properties of Quantum Spacetime, Phys. Rev. Lett. **102**, 111303 (2009).
[14] E. Alesci and M. Arzano, Anomalous dimension in three-dimensional semiclassical gravity, Phys. Lett. B **707**, 272 (2012).
[15] M. Arzano and T. Trzesniewski, Diffusion on κ-Minkowski space, Phys. Rev. D **89**, 124024 (2014).
[16] L. Modesto, Fractal spacetime from the area spectrum, Classical Quantum Gravity **26**, 242002 (2009).
[17] G. Calcagni, D. Oriti, and J. Thürigen, Dimensional flow in discrete quantum geometries, Phys. Rev. D **91**, 084047 (2015).
[18] J. Ambjorn, A. Görlich, J. Jurkiewicz, and R. Loll, Non-perturbative quantum gravity, Phys. Rep. **519**, 127 (2012).
[19] F. Dowker, Introduction to causal sets and their phenomenology, Gen. Relativ. Gravit. **45**, 1651 (2013).

[20] A. Eichhorn and S. Mizera, Spectral dimension in causal set quantum gravity, Classical Quantum Gravity **31**, 125007 (2014).
[21] A. Eichhorn, S. Mizera, and S. Surya, Echoes of asymptotic silence in causal set quantum gravity, Classical Quantum Gravity **34**, 16LT01 (2017).
[22] G. Calcagni, Loop quantum cosmology from group field theory, Phys. Rev. D **90**, 064047 (2014).
[23] G. Amelino-Camelia, M. Arzano, G. Gubitosi, and J. Magueijo, Dimensional reduction in the sky, Phys. Rev. D **87**, 123532 (2013).
[24] A. Pérez, The spin-foam approach to quantum gravity, Living Rev. Relativity **16**, 3 (2013).
[25] J. F. Plebanski, On the separation of Einsteinian substructures, J. Math. Phys. (N.Y.) **18**, 2511 (1977).
[26] G. T. Horowitz, Exactly soluble diffeomorphism invariant theories, Commun. Math. Phys. **125**, 417 (1989).
[27] J. W. Barrett and L. Crane, Relativistic spin networks and quantum gravity, J. Math. Phys. (N.Y.) **39**, 3296 (1998).
[28] J. W. Barrett and L. Crane, A Lorentzian signature model for quantum general relativity, Classical Quantum Gravity **17**, 3101 (2000).
[29] J. Engle, R. Pereira, and C. Rovelli, Loop-Quantum-Gravity Vertex Amplitude, Phys. Rev. Lett. **99**, 161301 (2007).
[30] J. Engle, R. Pereira, and C. Rovelli, Flipped spin-foam vertex and loop gravity, Nucl. Phys. **B798**, 251 (2008).
[31] J. Engle, E. R. Livine, R. Pereira, and C. Rovelli, LQG vertex with finite Immirzi parameter, Nucl. Phys. **B799**, 136 (2008).
[32] L. Freidel and K. Krasnov, A new spin-foam model for four-dimensional gravity, Classical Quantum Gravity **25**, 125018 (2008).
[33] A. Baratin and D. Oriti, Group field theory and simplicial gravity path integrals: A model for Holst-Plebanski gravity, Phys. Rev. D **85**, 044003 (2012).
[34] J. W. Barrett, R. J. Dowdall, W. J. Fairbairn, H. Gomes, F. Hellmann, and R. Pereira, Asymptotics of four-dimensional spin-foam models, Gen. Relativ. Gravit. **43**, 2421 (2011).
[35] D. Oriti, Group field theory and loop quantum gravity, in *Loop Quantum Gravity, 100 Years of General Relativity*, edited by A. Ashtekar (World Scientific, Singapore, 2017), pp. 125–151.
[36] L. Freidel, Group field theory: An overview, Int. J. Theor. Phys. **44**, 1769 (2005).
[37] D. Oriti, The group field theory approach to quantum gravity, in *Approaches to Quantum Gravity: Toward a New Understanding of Space, Time and Matter*, edited by D. Oriti (Cambridge University Press, Cambridge, 2007).
[38] D. Oriti, The microscopic dynamics of quantum space as a group field theory, in *Foundations of Space and Time* (Cambridge University Press, Cambridge, 2012).
[39] B. Dittrich, The continuum limit of loop quantum gravity: A framework for solving the theory, in *Loop Quantum Gravity, 100 Years of General Relativity*, edited by A. Ashtekar (World Scientific, Singapore, 2017), pp. 153–179.
[40] B. Dittrich, From the discrete to the continuous: Towards a cylindrically consistent dynamics, New J. Phys. **14**, 123004 (2012).
[41] B. Dittrich, F. C. Eckert, and M. Martin-Benito, Coarse graining methods for spin net and spin-foam models, New J. Phys. **14**, 035008 (2012).
[42] B. Dittrich, E. Schnetter, C. J. Seth, and S. Steinhaus, Coarse graining flow of spin-foam intertwiners, Phys. Rev. D **94**, 124050 (2016).
[43] B. Bahr and S. Steinhaus, Investigation of the spin-foam path integral with quantum cuboid intertwiners, Phys. Rev. D **93**, 104029 (2016).
[44] B. Bahr and S. Steinhaus, Numerical evidence for a phase transition in four-dimensional spin-foam quantum gravity, New J. Phys. **14**, 035008 (2012).
[45] B. Bahr and S. Steinhaus, Hypercuboidal renormalization in spin-foam quantum gravity, Phys. Rev. D **95**, 126006 (2017).
[46] E. R. Livine and S. Speziale, New spin-foam vertex for quantum gravity, Phys. Rev. D **76**, 084028 (2007).
[47] B. Bahr, S. Klöser, and G. Rabuffo, Towards a cosmological subsector of spin-foam quantum gravity, Phys. Rev. D **96**, 086009 (2017).
[48] B. Dittrich and S. Steinhaus, Time evolution as refining, coarse graining, and entangling, New J. Phys. **16**, 123041 (2014).
[49] H. Sahlmann, Wave propagation on a random lattice, Phys. Rev. D **82**, 064018 (2010).
[50] W. Kaminski, M. Kisielowski, and J. Lewandowski, Spin foams for all loop quantum gravity, Classical Quantum Gravity **27**, 095006 (2010).
[51] H. W. Hamber and R. M. Williams, On the measure in simplicial gravity, Phys. Rev. D **59**, 064014 (1999).
[52] P. Menotti and P. P. Peirano, Diffeomorphism invariant measure for finite dimensional geometries, Nucl. Phys. **B488**, 719 (1997).
[53] B. Dittrich and S. Steinhaus, Path integral measure and triangulation independence in discrete gravity, Phys. Rev. D **85**, 044032 (2012).
[54] A. Ashtekar and C. J. Isham, Representations of the holonomy algebras of gravity and non-Abelian gauge theories, Classical Quantum Gravity **9**, 1433 (1992).
[55] A. Ashtekar and J. Lewandowski, Projective techniques and functional integration for gauge theories, J. Math. Phys. (N.Y.) **36**, 2170 (1995).
[56] F. Conrady and L. Freidel, On the semiclassical limit of four-dimensional spin-foam models, Phys. Rev. D **78**, 104023 (2008).
[57] J. W. Barrett, R. J. Dowdall, W. J. Fairbairn, H. Gomes, and F. Hellmann, Asymptotic analysis of the Engle-Pereira-Rovelli-Livine four-simplex amplitude, J. Math. Phys. (N.Y.) **50**, 112504 (2009).
[58] J. W. Barrett, R. J. Dowdall, W. J. Fairbairn, F. Hellmann, and R. Pereira, Lorentzian spin-foam amplitudes: Graphical calculus and asymptotics, Classical Quantum Gravity **27**, 165009 (2010).
[59] P. Don, M. Fanizza, G. Sarno, and S. Speziale, SU(2) graph invariants, Regge actions and polytopes, Classical Quantum Gravity **35**, 045011 (2018).
[60] L. Freidel and S. Speziale, Twisted geometries: A geometric parametrization of SU(2) phase space, Phys. Rev. D **82**, 084040 (2010).
[61] V. Belov, Poincaré-Plebański formulation of GR and dual simplicity constraints, Phys. Rev. D **82**, 084040 (2010).

[62] G. Calcagni, D. Oriti, and J. Thürigen, Laplacians on discrete and quantum geometries, Classical Quantum Gravity **30**, 125006 (2013).
[63] E. R. Livine and J. P. Ryan, A note on B-observables in Ponzano Regge three-dimensional quantum gravity, Classical Quantum Gravity **26**, 035013 (2009).
[64] J. W. Barrett, M. Rocek, and R. M. Williams, A note on area variables in Regge calculus, Classical Quantum Gravity **16**, 1373 (1999).
[65] A. Baratin, B. Dittrich, D. Oriti, and J. Tambornino, Non-commutative flux representation for loop quantum gravity, Classical Quantum Gravity **28**, 175011 (2011).
[66] B. Dittrich and S. Speziale, Area-angle variables for general relativity, New J. Phys. **10**, 083006 (2008).
[67] J. Thürigen, Discrete quantum geometries and their effective dimension, Ph.D. thesis, Humboldt-Universität zu Berlin, 2015.
[68] G. Calcagni, D. Oriti, and J. Thürigen, Spectral dimension of quantum geometries, Classical Quantum Gravity **31**, 135014 (2014).
[69] J. D. Christensen and G. Egan, An efficient algorithm for the Riemannian 10j symbols, Classical Quantum Gravity **19**, 1185 (2002).
[70] T. Hahn, The CUBA library, Nucl. Instrum. Methods Phys. Res., Sect. A **559**, 273 (2006).
[71] L. Smolin, Linking topological quantum field theory and nonperturbative quantum gravity, J. Math. Phys. (N.Y.) **36**, 6417 (1995).
[72] S. Major and L. Smolin, Quantum deformation of quantum gravity, Nucl. Phys. **B473**, 267 (1996).
[73] R. Borissov, S. Major, and L. Smolin, The geometry of quantum spin networks, Classical Quantum Gravity **13**, 3183 (1996).
[74] K. Noui and P. Roche, Cosmological deformation of Lorentzian spin-foam models, Classical Quantum Gravity **20**, 3175 (2003).
[75] W. J. Fairbairn and C. Meusburger, Quantum deformation of two four-dimensional spin-foam models, J. Math. Phys. (N.Y.) **53**, 022501 (2012).
[76] M. Han, Four-dimensional spin-foam model with quantum Lorentz group, J. Math. Phys. (N.Y.) **52**, 072501 (2011).
[77] V. G. Turaev and O. Y. Viro, State sum invariants of 3 manifolds and quantum 6j symbols, Topology **31**, 865 (1992).
[78] H. M. Haggard, M. Han, W. Kaminski, and A. Riello, SL(2,C) ChernSimons theory, a nonplanar graph operator, and four-dimensional quantum gravity with a cosmological constant: Semiclassical geometry, Nucl. Phys. **B900**, 1 (2015).
[79] B. Bahr and B. Dittrich, Breaking and restoring of diffeomorphism symmetry in discrete gravity, AIP Conf. Proc. **1196**, 10 (2009).
[80] B. Bahr, B. Dittrich, and S. Steinhaus, Perfect discretization of reparametrization invariant path integrals, Phys. Rev. D **83**, 105026 (2011).
[81] G. Calcagni, Complex dimensions and their observability, Phys. Rev. D **96**, 046001 (2017).
[82] V. Bonzom, Large N limits in tensor models: Towards more universality classes of colored triangulations in dimension $d \geq 2$, SIGMA **12**, 073 (2016).
[83] L. Lionni and J. Thürigen, Multicritical behavior of four-dimensional tensor models up to order 6, Phys. Rev. D **83**, 105026 (2011).
[84] R. Gurau, *Random Tensors* (Oxford University Press, Oxford, 2016).
[85] R. Gurau and J. P. Ryan, Colored Tensor Models—a Review, SIGMA **8**, 020 (2012).
[86] V. Bonzom, R. Gurau, A. Riello, and V. Rivasseau, Critical behavior of colored tensor models in the large N limit, Nucl. Phys. **B853**, 174 (2011).
[87] R. Gurau and J. P. Ryan, Melons are branched polymers, Ann. Henri Poincaré **15**, 2085 (2014).
[88] B. Bahr and G. Rabuffo, Deformation of the EPRL spin-foam model by a cosmological constant, arXiv:1803.0183.